What Drives Plate Motions?

Yongfeng Yang

Bureau of Water Resources of Shandong Province, Jinan, China

Abstract

Plate motion was widely ascribed to several driving forces like ridge push, slab pull, and basal drag. However, an in-depth investigation shows these forces incomplete. Here we propose, the oceans generate varying unequal pressures everywhere, the application of these pressures to the entire sides of continents create enormous horizontal forces (i.e., the ocean-generating forces), the net effect of these forces provides lateral push to the continents and may cause them to move horizontally, further, the travelling continents drag the crusts they connect to move, these totally form plate motion. A roughly estimation shows that the ocean-generating forces may give South American, African, Indian, and Australian continents a movement of respectively 2.8, 4.2, 5.7, and 6.3 cm/yr, and give Pacific Plate a movement of 8.9 cm/yr. Some torque effects of the ocean-generating forces contribute to rotate North American and Eurasian continents.

1 Introduction

One of the most significantly achievements in the 20th century was the establishment of plate tectonics that developed from a previous conception of continental drift. The continent drift theory hypothesized that the continents had slowly floated over the Earth's surface in the distant past (Wegener, 1915 and 1924). The evidences supporting this surface motion include a shape fitting at the opposed sides of African and American continents, coal belt crossed

from North American to Eurasian, identical direction of ice sheet of southern Africa and India, and speed measurement made by global positioning system (GPS). In addition, the discovery of paleomagnetic reversals in oceans, which reflects seafloor spreading, further consolidated the belief of Earth's surface motion (Hess, 1962; Vine and Matthews, 1963). Nevertheless, the driving force for this surface motion always remains poorly understood. The first to consider the dynamics source of this motion is the contraction theory, which proposed that a wrinkling process of Earth's surface had forced the Himalayas to climb up. Wegener (1915) directly ascribed continent's drift to the centrifugal and tidal forces, these forces were latterly found to be too weak to work. For instance, Jeffreys (1929) estimated that the mean tidal friction slowing the Earth's rotation corresponds to a westward stress of the order of only 10^{-4} dyn/cm^2 over the Earth's surface, this stress is too small to maintain that drift. After these attempts failed, people turned their eyes to the interior of the Earth to seek for the answer, together with the rebirth of the continental drift theory in the form of 'plate tectonics', this eventually fostered a series of various driving forces like ridge push, slab pull, basal drag, slab suction, the geoid's deformation, and the Coriolis force to account for plate motion (Holmes, 1931; Runcorn, 1962a, b; Turcotte and Oxburgh, 1972; Oxburgh and Turcotte, 1978; Spence, 1987; White & McKenzie, 1989; Conrad & Lithgow-Bertelloni, 2002). Of these driving forces, the geoid's deformation is almost symmetrical relative to the Earth's shape, the Coriolis force is symmetrical relative to equator, they may be easily excluded. Slab suction occurs when local mantle currents exert a downward pull on nearby plates in the subduction zone (McKenzie, 1969; Sleep & Toksoz, 1971; Elsasser, 1971; Richter, 1973), but its nature is unclear (Forsyth & Uyeda, 1975; Conrad & Lithgow-Bertelloni, 2002). Finally, ridge push, slab pull, and basal drag are left to be the driving forces for plate motion. A strictly investigation, however, reveals that there are too many uncertainties for these forces.

Ridge push. Ridge push was caused by the potential energy gradient from the raised oceanic lithosphere. Forsyth & Uyeda (1975) initially defined it as an edge force, from then on, it has been recognized as a force to drive plate (Hager and O'Connell, 1981; Spence, 1987; White & McKenzie, 1989; Turcotte and Schubert, 2002). Nevertheless, there are two aspects to

discount ridge push. On the one hand, the inclusion of this force is entirely speculative. According to the seminal work of Forsyth & Uyeda (1975), the authors found a striking correlation between plate's velocity and length of trench with subducted slab and then proposed slab pull as a driving force, but since plates having no downgoing slabs are also moving, this discrepancy makes them conceive of a push from the ridge to replace slab pull. In fact, as pointed out by these authors, there is no evidence to show a coupling of plate motion and length of ridge. On the other hand, all the plates are steadily moving over the Earth's surface, naturally, a plate would ride onto another plate in the front and depart from a third plate in the rear. The department would result in fracture between the two plates. The fracture, if deep enough to contact the asthenosphere, would allow magma to erupt and form Mid-Oceanic Ridge (MOR). From this perspective, the MOR itself may be the result of plate motion. In fact, Wilson and Burke (1973) had pointed out that the ridges may originally have formed as a passive consequence of the plates moving apart. But nowadays, the MOR are conversely treated as a cause to yield push force to further drive plate. This goes to the notorious chicken-or-egg question, who is the first? In physical field, it is required that a movement (i.e., result) must be clearly separated from the force (i.e., cause) that sustains it. In the section of discussion of this work, we shall further demonstrate how ridge push is not consistent with globally stress observation.

Slab pull. Slab pull was caused by a cold, dense sinking plate that uses its own weight to pull the remaining plate it attaches (Forsyth & Uyeda, 1975; Conrad and Lithgow-Bertelloni, 2002). Similar to the matter of ridge push, this force is inconclusively established. According to Forsyth & Uyeda (1975), the selected 12 plates may be apparently divided into two groups: these that connect to downgoing slabs are all moving at 6-9 cm/yr relative to the mantle, and those that have no downgoing slabs are moving at 0 to 4 cm/yr. Forsyth & Uyeda inferred from the correlation between plate's velocity and length of trench with subducted slab that there is a fundamental difference in the forces acting on these two sets of plates, and further concluded that the presence or absence of a downgoing slab is a dominating factor for this difference. This conclusion, however, is not dependable. For example, there are two groups of

buses, one group hold male passengers and run slowly, another group hold female passengers and run rapidly, a statistic analysis then shows that there is a striking correlation between bus's velocity and passenger's gender. It is true that we cannot use this correlation to draw a conclusion that the gender difference of passenger is a dominating factor for the difference in the forces acting on these two groups of buses. The 12 selected plates may resemble the buses, of these, the downgoing slabs of these plates may resemble the female passengers, the continents of these plates may resemble the male passengers. Actually, we may have explanation for the correlation of plate's velocity and length of trench. For instance, these plates connecting to downgoing slabs are generally oceanic, while those plates having no downgoing slabs are generally continental, the oceanic plates are geographically lower than the continental plates, since the plates are all moving around the Earth's surface, this altitude difference makes the oceanic plates easily subduct into the continental plates. From this viewpoint, the downgoing slabs are the result of plate motion and irrelevant to plate's velocity. This also returns to the chicken-or-egg question we mentioned above, who is the first? Some authors (e.g., Knopoff ,1972; Minster et al. 1974) ascribed the velocity difference between the oceanic and continental plates to the mantle drag that is weak under oceanic plates but strong under continents. Forsyth & Uyeda (1975) argued that the basal drag difference cannot provide an explanation for the narrow range of velocities of the oceanic plates. Our concern lies at, except for slab pull, this narrow range of velocities may be formed through other way. For example, since the oceanic plates are directly or indirectly connected to each other, such a physical binding will constrain them to follow a similar manner of movement, in which an approach of velocity is possible.

Basal drag. Basal drag originates from mantle dynamics and was caused by the viscous moving asthenosphere along the bottom of lithosphere (Holmes, 1931; Pekeris, 1935; Hales, 1936; Runcorn, 1962a, b; Turcotte and Oxburgh, 1972; Oxburgh and Turcotte, 1978; Tanimoto & Lay, 2000; Bercovici, et al., 2015). Nevertheless, there are many uncertainties for this force. First of all, the mantle dynamics itself has been long disputed. The cells proposed to exist in the asthenosphere require strong fitting to plate size. Seismic tomography showed

that rising mantle material beneath ridges only extends down 200 to 400 km (Foulger, et al., 2001). This depth gives an upper limitation on the scale of the proposed cells. Most of plates (South American, North American, Eurasian, and Pacific, for instance) hold a width of generally more than thousands of kilometers, such a width is far greater than the scale of the proposed cells. Foster (1969) demonstrated that the scale of the proposed cells may be even smaller in the high Rayleigh number range. Forsyth & Uyeda (1975) pointed out, small cells can provide only a little net contribution to plate motion when integrated over the entire area of plate. Additionally, the toroidal motion proposed by mantle dynamics undertakes horizontal rotation (Bercovic, et al., 2015). The generation of torioidal motion requires variable viscosity, but unfortunately, numerous studies of basic 3-D convection with temperature-dependent viscosity had failed to yield the requisite toroidal flow (Bercovic, 1993, 1995b; Cadek et al., 1993; Christensen and Harder, 1991; Tackley, 1998; Trompert and Hansen, 1998; Weinstein, 1998; Stein et al., 2004). Second, according to Forsyth & Uyeda (1975), there is no evidence to show a correlation between plate velocity and surface area. This lack suggests that basal drag cannot be a driving force. Some authors argued that the contribution of basal drag to plate motion depends on the flow pattern at the lithosphere mantle interface (Forsyth and Uyeda, 1975; Doglioni, 1990), but the nature of this interface and its flow pattern are unclear. Last, both modeling works (e.g., Richter, 1973; Richardson and Cox, 1984; Turcotte and Schubert, 2002) and globally tectonic stress measurements (e.g., Ranalli and Chandler, 1975; Zoback et al., 1989; Zoback, 1992) trended to agree that the viscous asthenosphere provides resistence rather than driving to plate motion.

Besides these uncertainties mentioned, there are still many challenges for these driving forces. For example, some plates (South American, African, and Indian-Australian) move approximately along straight path, while others (Eurasian and North American) move in a rotating way. Most strangely, Indian-Australian and Pacific plates move nearly orthogonal to each other. It is considerably difficult to imagine how these forces work together to manage these various surface motions. Additionally, these forces are also unsuccessful in yielding plate motions, although some models had yielded plate-like behavior and mathematically got

solution for plate's velocity by means of a non-Newtonian way, i.e., a balance relationship of buoyancy force and drag force (Bercovici, et al., 2015). Furthermore, other problems like changes in plate motion, plateness, and asymmetry of subduction remains unresolved in the paradigms of these driving forces (Bercovici, et al., 2015). In fact, if these driving forces are packaged to be considered, readers can find another problem. Ridge push arises from the raised oceanic lithosphere, slab pull arises from the downgoing slab, these sequences of process require the ridge and downging slab itself to form earlier than ridge push and slab pull, respectively. And then, a following question will be who initially supplied energy to create the ridge and downgoing slab. If our understanding is restricted to a circle of these driving forces, it is necessary to ascribe this source to mantle dynamics. Subsequently, so long as mantle dynamics is falsified, the ridge push and slab pull would become rootless. The uncertainties of mantle dynamics mentioned above are undoubtedly weakening the foundation of ridge push and slab pull.

For almost one hundred of years, the exploration on the dynamic source of plate motion has been always intensive among scientists. Since 1970's, some had begun to evaluate the relative importance of these driving forces (Forsyth & Uyeda, 1975; Backus, et al., 1981; Bokelmann, 2002). These efforts give people a sense that all the forces related to plate motion had been found. The fact, however, is not so, another force has been neglected. In this work, we get back to the exterior of the Earth to seek this force and consider a solution for plate motion.

2 An ocean-generating force driving mechanism for plate motion

2.1 Forces acting on continent

Liquid exerts pressure at the side of a vessel that holds it. Refer to the top of Figure 1, the pressure at the side of a cubic vessel may be written as $P=\rho g y/2$, the application of this pressure over the side generates force for the vessel, this force may be expressed as $F=PS=\rho g y^2 x/2$, where S is the side's area, ρ, g, x, and y are respectively density of liquid, gravitational acceleration, vessel's width, and liquid's depth. Get back to real world, ocean

basins are naturally gigantic vessels, their depths are usually more than a few kilometers, furthermore, these depths vary from one place to another. All these determine that oceans are yielding enormous unequal pressures nowhere. Most of oceans experience two cycles of high and low water per day, this oscillation often holds an amplitude of a few meters, these are the tides we know in everyday life. Related to the expression above, the addition of tides to oceans is yielding enormous varying unequal pressures, and further, the application of these pressures over the continent's sides may generate enormous unequal forces. Ocean pressure variations had been confirmed by means of bottom pressure measurements around the globe (Fig. 2). The results of bottom pressure measurements reveal that ocean pressure variations not only closely relate to the daily tides but also greatly differ from one ocean to another. For example, at the time of new Moon the range of bottom pressure variation at North Santo Domingo (Atlantic ocean) is almost within 100 millibars, while at South Dutch Harbor (Pacific ocean) this range may reach up to 260 millibars. Ocean pressure exerts always orthogonal to the continental slope, by which a normal force is formed. Geometrically, this normal force can further be decomposed into a horizontal force and a vertical force. We here define the continental crust, which has been applied by ocean pressure, as continent in the following sections. In the following, we list the plausible forces acting on the continent as illustrated in Figure 1 and discuss the physical nature of these forces. The forces acting on continents can be classified into two categories: the forces acting at the parts of continent that connect to ocean, and those acting at both the bottom surface of continent and the parts of continent that connect to adjacent crusts. The forces acting at the parts of continent that connect to ocean originate from ocean pressures. They will be called horizontal forces and denoted F_L' at the right and F_R' at the left. The force acting at the bottom surface of continent arises from a viscous coupling between the continent and underlying asthenosphere. It will be called basal friction force and denoted f_{base}. As addressed by Forsyth & Uyeda (1975), if there is an active flow in the asthenosphere, such as thermal convection, f_{base} will act as a driving force (Runcorn, 1962a, b; Morgan, 1972; Turcotte & Oxburgh, 1972). If, on the other hand, the asthenosphere is passive with regard to the plate motion, f_{base} will be resistive force. We

here accept f_{base} as resistive force. The forces acting at the parts of continent that connect to adjacent crusts arise from a physical binding between the continent and adjacent crusts, given the continent moves towards right, they will be called push force from the crust at the right side, pull force from the crust at the left side, shearing force from the crust at the far side, and shearing force from the crust at the near side, and denoted f_{right}, f_{left}, f_{far}, and f_{near}, respectively. It is important to note that, if there were no fractures (the gaps along the ocean ridges, for instance) within ocean basin, the horizontal forces generated at the sides of ocean basin (these sides are also the sides of continent) would be entirely balanced by the basin itself, this makes these horizontal forces unable to interact with the basal friction force. Forsyth & Uyeda (1975) showed that the total length of all the world's extensional boundaries (representing the fractures) may reach up to 50,000 km. The existence of these fractures of ocean basins allows the horizontal force generated to interact with the basal friction exerted by the asthenosphere. And then, a combination of all these forces for the continent may be written as

$$F = (F_L' - F_R') - (f_{base} + f_{right} + f_{left} + f_{far} + f_{near}) \quad (1)$$

where the first term ($F_L' - F_R'$) denotes the net horizontal force that provides a dynamic source for the continent, the second term ($f_{base} + f_{right} + f_{left} + f_{far} + f_{near}$) denotes the total resistive force that attempts to hinder the continent's movement. F_L' and F_R' may be further written as $F_L'=0.5\rho g L(h_L+h_L')^2$, $F_R'=0.5\rho g L(h_R+h_R')^2$, and ρ, g, L, h_L, and h_R are respectively density of water, gravitational acceleration, ocean's width that corresponds to the continent's width, ocean's depth at the left, and ocean's depth at the right, h_L' and h_R' are respectively the tidal heights at both sides. The tidal heights can be expressed as $h_L'=A_L\sin\omega t$, and $h_R'=A_R\sin(\omega t+\varphi)$, A_L and A_R are tidal amplitudes, ω, t, and φ are respectively angular frequency, time, and phase difference between the tides at both sides of the continent.

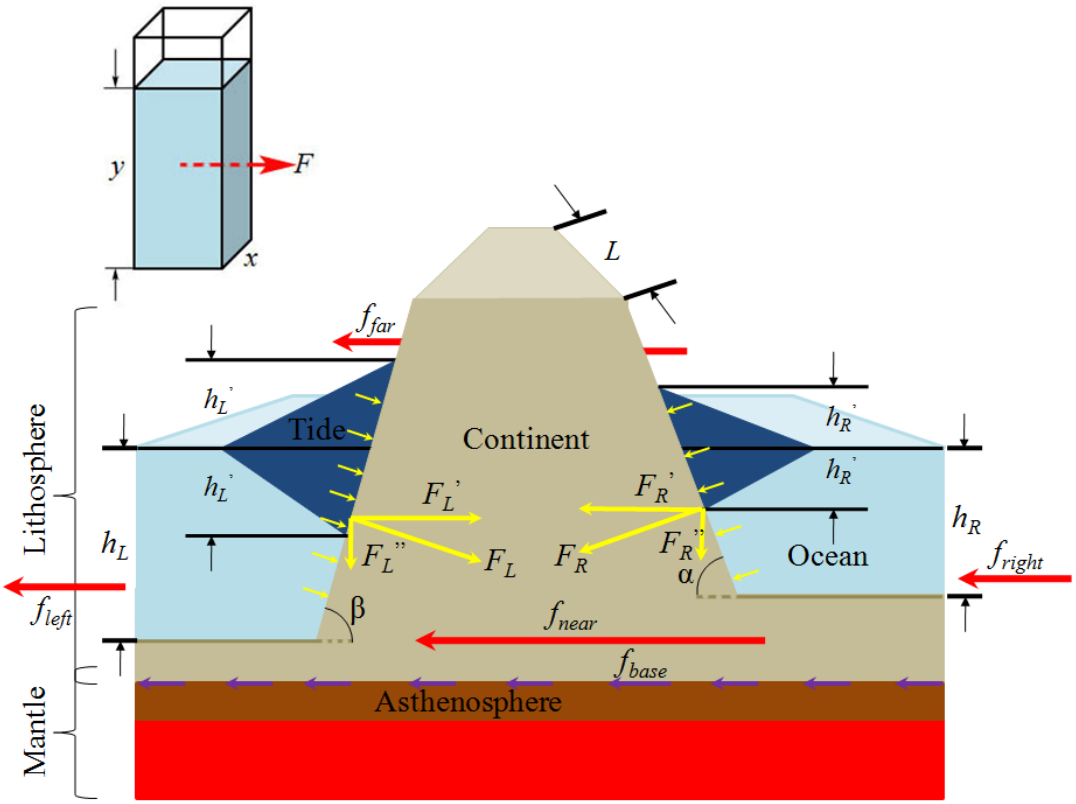

Fig. 1. Modelling the dynamics of continent. $F_L(F_R)$ represents the normal force generated due to ocean pressure at the left (right) side of the continent, while $F_L'(F_R')$ and $F_L''(F_R'')$ denote respectively the horizontal and vertical forces decomposed from that normal force. f_{base} denotes basal friction force exerted by the asthenosphere, while f_{right}, f_{left}, f_{far}, and f_{near} denote the push force from the crust at the right side, the pull force from the crust at the left side, the shearing force from the crust at the far side, and the shearing force from the crust at the near side of the continent. L denotes the width of the continent's side, h_L and h_R are respectively ocean's depth at the left and at the right, h_L' and h_R' are the tidal heights at both sides. α and β denote the inclinations of the continent's slope at both sides. Note that the tidal heights are highly exaggerated relative to ocean depth.

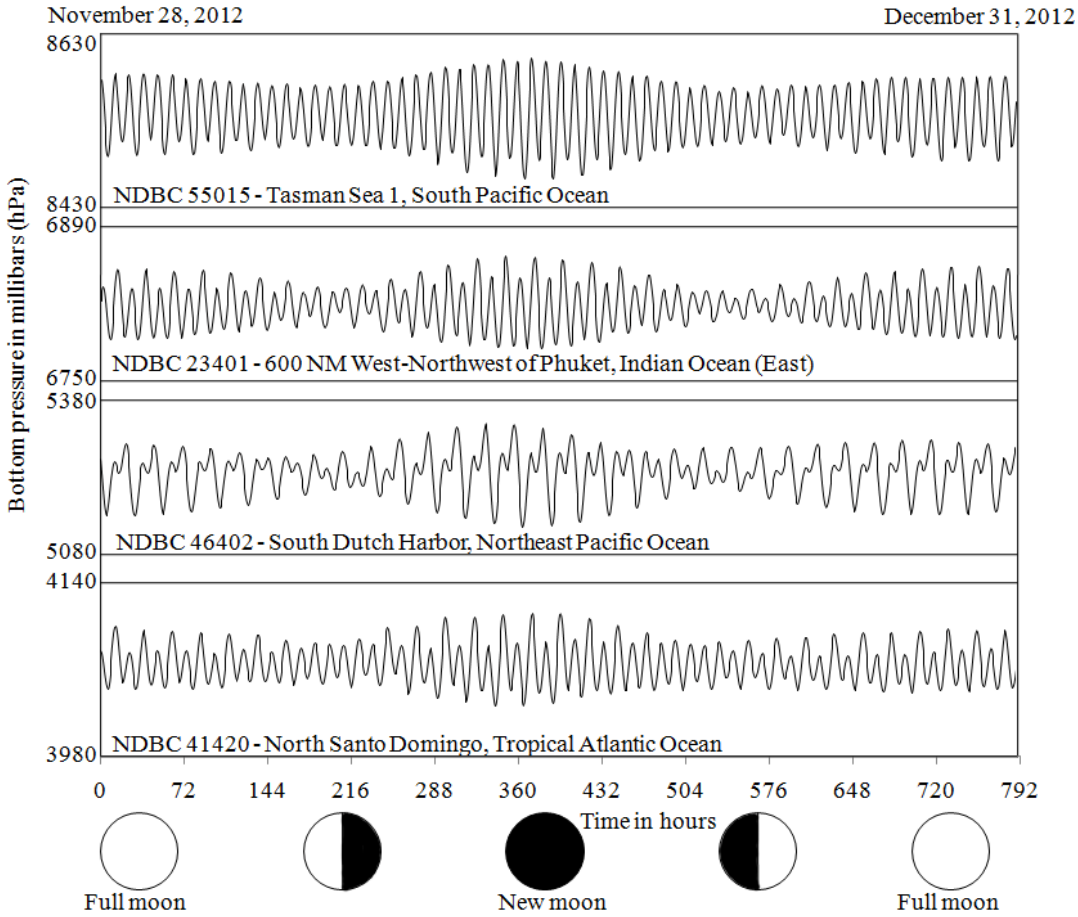

Fig. 2. Typical 1-month bottom pressure records from Pacific, Atlantic, and Indian oceans during 2012. Bottom pressure record data are from PSMSL (Permanent Service for Mean Sea Level).

2.2 Continent's movement

The equation (1) provides three possibilities for the continent. If the net horizontal force is less than or equal to the total resistive force, it means the net horizontal force cannot overcome the total resistive force; If the net horizontal force is greater than the total resistive force, it means the net horizontal force can overcome the total resistive force, the continent gets a lasting net force; And if the net horizontal force is sometime greater than the total resistive force but sometime less than the total resistive force, it means the continent gets a discontinuous net force. As a lasting force can yield an accelerative movement for an object, it is impossible for the continent to own such a force. We here allow the continent to get a

discontinuous force. To clarify the following deduction, we divide the net horizontal force (F_L'- F_R') into two parts: the horizontal force generated due to ocean (denoted F_{ocean}) and the horizontal force generated due to tide (denoted F_{tide}), and assume that the total resistive force (denoted $F_{resistive}$) is constant and its magnitude is slightly less than the maximum net horizontal force. The maximum net horizontal force arises from the oscillation of ocean that is related to tide. Under the effect of a discontinuous force, the continent's movement may be described as below: refer to Figure 3, at the stage of t_1, the net horizontal force begins to increase as the tidal height increases, but since $(F_{ocean}+F_{tide})-F_{resistive}<0$, the continent remains motionless; At the stage of t_2, $(F_{ocean}+F_{tide})-F_{resistive}>0$, the continent accelerates to move, and its speed reaches a high level at the end of this period; At the stage of t_3, $(F_{ocean}+F_{tide})-F_{resistive}<0$, the continent begins to decelerate until its speed becomes zero at the end of this period; At the stage of t_4, due to $(F_{ocean}+F_{tide})-F_{resistive}<0$, the continent remains motionless; And at the stage of t_5 and t_6, the continent obtains a movement that is similar to the movement at the stage of t_2 and t_3, but at the stage of t_7, the continent again remains motionless. Simply, the continent discontinuously obtains some movements at the stages of t_2, t_3, t_5, and t_6, and some stagnations at the stages of t_1, t_4, and t_7. These processes totally provide a net forward movement for the continent during the day. Expanding this day to the whole year, it indicates that the continent obtains a steadily movement during the year. Further, extending this year to a long timescale of millions of years and to the fact that the tides are extensively distributed around the globe, we conclude that the continents had obtained steadily movements over millions of years. Figure 4 exhibits a globally distribution of the tides and the horizontal forces generated due to oceans.

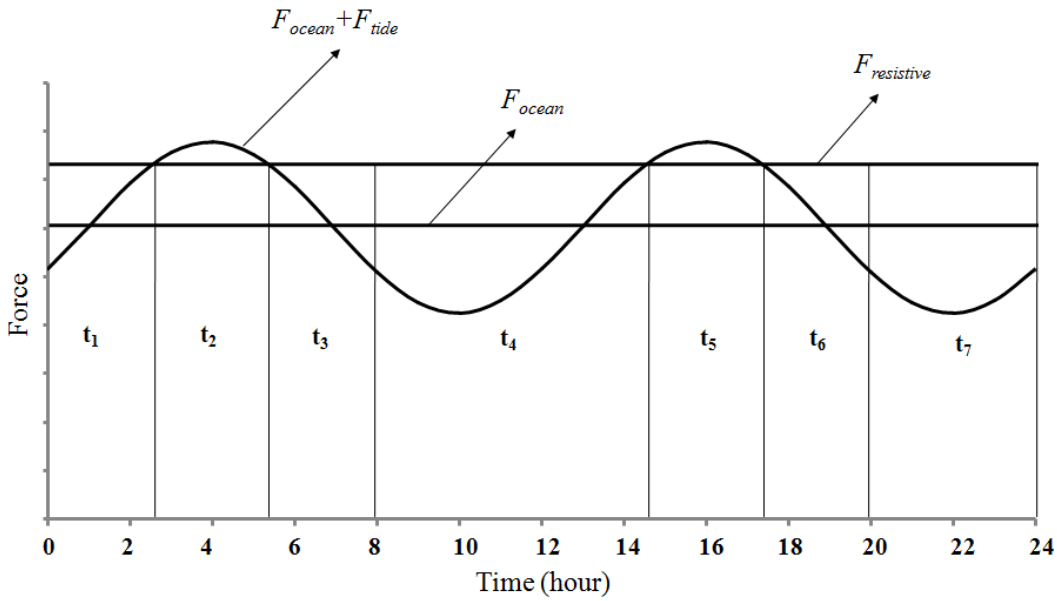

Fig. 3. Dynamic analysis for continent. $F_{ocean} + F_{tide}$ denote the net horizontal force generated, $F_{resistive}$ denotes the total resistive force. Note that the oscillation of the net horizontal force is exceedingly exaggerated.

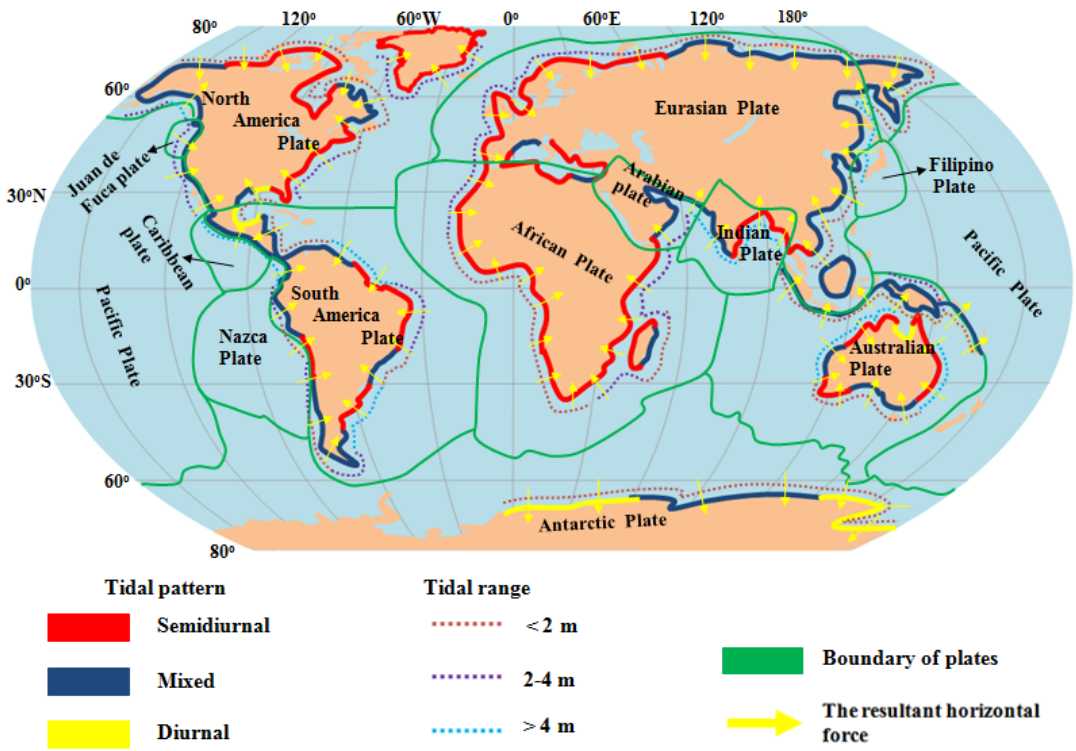

Fig. 4. A global view of the distribution of tidal pattern, tidal range, plate tectonics, and the resultant horizontally forces from ocean. Tide data supporting is from U.S. NOAA, GLOSS database - University of Hawaii Sea Level Center (Caldwell et al. 2015), and Bureau National

Operations Centre (BNOC) of Australia, and tide range also refer to the times atlas of the oceans, 1983, Van Nostrand Reinhold, NY.

A quantitative treatment of the continent's movement must include more details. Practically, a continent, if not connected to another, is being surrounded by oceans, this means that the net horizontal force accepted by this continent would be a combination of the horizontal forces generated at all the sides of the continent. The spherical Earth makes the horizontal forces generated unable to fall onto a plane. In addition, the tides are not synchronous in the oceans, their amplitudes perform two cycles per month, which are related to the positions of the Sun, Moon, and Earth, and become maximal at the times of full and new Moon and minimum at the times of first quarter and last quarter. Furthermore, the loading/unloading rate of tide is not uniform, this leads the horizontal force generated to vary, a changing rate yields difficulty in determining the time that the continent takes to accelerate and decelerate during a tide. More features of the tides may refer to these works (Pugh 1987; Pugh and Woodworth 2014). To simplify the calculation below, the continent is firstly assumed to be more rigid and planar, this allows Newton's mechanics to be used to determine the continent's movement. We further assume all the tides that circle the continent to be synchronous and the amplitudes of these tides to be constant. Based on equation (1), the net horizontal force generated would be maximal when the phase difference (φ) between the tides at both sides is 90°, whereas minimal when the phase difference (φ) is 0°. The synchronous represents the phase difference (φ) is 0°. It may be inferred, if the net horizontal force generated under this condition (i.e., the phase difference $\varphi=0^o$) is greater than total resistive force, naturally, the net horizontal force generated under other condition (the phase difference $\varphi\neq0^o$) is greater than the total resistive force. We thus use the net horizontal force generated under the condition when the phase difference (φ) is equal to zero to acts as a lowest threshold to determine the continent's movement. We further assume the loading/unloading rate of tide to be uniform, if correlated with Figure 3, this indicates that the time the continents takes to accelerate is equal to the time it takes to decelerate during a tide, namely, $t_2=t_3$. And then, according to the knowledge of

Newton's 2nd law, the movement that a continent obtains during a year may be approximately written as

$$D = \mathbf{365} * \mathbf{2} * (\frac{1}{2} * \left(\frac{1}{2} * \frac{\left(F_{ocean} + F_{\mathbf{max}-tide} - F_{resistive}\right)}{M} \right) * t^{\mathbf{2}} + (\frac{1}{2} * \frac{\left(F_{ocean} + F_{\mathbf{max}-tide} - F_{resistive}\right)}{M} * t) * t$$
$$-\frac{1}{2} * \left(\frac{1}{2} * \frac{\left(F_{resistive} - F_{ocean} - F_{\mathbf{max}-tide} * \mathbf{cos}\left(\frac{3}{2} * \omega t\right)\right)}{M} \right) * t^{\mathbf{2}})$$

(2)

where (F_{ocean}+ $F_{max\text{-}tide}$) denotes the maximum net horizontal force generated, F_{ocean} denotes the total horizontal force generated due to ocean and may be written as $F_{ocean} = \left((\sum_{i=1}^{n} F_{i-ocean-latitudinal})^{\mathbf{2}} + (\sum_{i=1}^{n} F_{i-ocean-longitudinal})^{\mathbf{2}} \right)^{\frac{1}{2}}$, $F_{i\text{-}ocean\text{-}latitudinal}$ and $F_{i\text{-}ocean\text{-}longitudinal}$ are respectively the latitudinal and longitudinal forces that are decomposed from the horizontal force generated at the *i*th side of a continent, they may be further written as $F_{i-ocean-latitudinal} = F_{i-ocean} \sin\Omega_i$, $F_{i-ocean-longitudinal} = F_{i-ocean} \cos\Omega_i$. $F_{i\text{-}ocean}$ denote the horizontal force generated due to ocean at the *i*th side of the continent and may be written as $F_{i-ocean} = \mathbf{0.5\rho g} L h_{\mathbf{ocean}}{}^{2}$. $F_{\max\text{-}tide}$ denotes the maximum total horizontal force generated due to tide and may be written as $F_{\max-tide} = \left((\sum_{i=1}^{n} F_{i-tide-latitudinal})^{\mathbf{2}} + (\sum_{i=1}^{n} F_{i-tide-longitudinal})^{\mathbf{2}} \right)^{\frac{1}{2}}$, $F_{i\text{-}tide\text{-}latitudinal}$ and $F_{i\text{-}tide\text{-}longitudinal}$ denote respectively the latitudinal and longitudinal forces that are decomposed from the horizontal force generated due to tide at the *i*th side of the continent, they may be expressed as $F_{i-tide-latitudinal} = F_{i-tide} \sin\Omega_i$, $F_{i-tide-longitudinal} = F_{i-tide} \cos\Omega_i$. $F_{i\text{-}tide}$ denotes the horizontal force generated due to tide at the *i*th side of a continent at the time of highest high tide and may be written as $F_{i-tide} = \mathbf{0.5\rho g} L \left(2 h_{\mathbf{ocean}} h_{\mathbf{tide}} + h_{\mathbf{tide}}{}^{2}\right)$. Ω_i denotes the inclination of

the ith side to latitude, it may be got through the geographic latitudes and longitudes of the two ends of this side. ρ, g, L, h_{ocean}, and h_{tide} are respectively density of water, gravitational acceleration, the continent side's width, ocean depth, and tidal height. M denotes the continent's mass and can be got through $M=S\text{d}\rho_{\text{continent}}$, where S, d, and $\rho_{\text{continent}}$ are respectively the continent's area, thickness, and density. $F_{resistive}$ denotes the total resistive force and is currently unknown, we have to value it in the calculation. ω is angular frequency, its magnitude is roughly equal to 30° per hour (equal to 0.00833° per second). t is the time that the continent takes to accelerate during a tide, subsequently, according to a relationship of movement, the time may be solved as

$$t = \frac{2}{3\omega}\arccos\left(\frac{2(F_{resistive} - F_{ocean})}{F_{\max-tide}} - 1\right) \tag{3}$$

Practically, the continent's side is not flat, and the continent's base is generally wider than its top, these make the continent look like a circular truncated cone staying in the ocean. As the horizontal force generated relates to the ocean's width (i.e., the continent side's width), we need to firstly project a continent along horizontal direction into a polygonal column and cut the side of this column into a series of smaller rectangular sides connecting one to another, and then, calculate the horizontal force generated at each of these rectangular sides, last, we combine these horizontal forces to form a single horizontal force. With these theoretical ideas, we take the parameters involved above to calculate the movements of a few continents (South American, African, Indian, and Australian). The controlling sites used to calculate the length of side refer to Figure 5, the longitudes and latitudes of these sites are resolved through Google Earth software. The given values for the parameters, the horizontal forces generated, and the resultant movements are respectively listed in table 1, 2, and 3. Overall, the resultant movements for South American, African, Indian, and Australian continents are respectively 2.8, 4.2, 5.7, and 6.3 cm/yr, which are well consistent with the observed movement of generally 5.0~10.0 cm/yr (Read and Watson 1975).

Careful readers would see, the total resistive force ($F_{resistive}$) we used in the calculation is technically valued. Such a treatment is needed. As shown in Figure 1, the total resistive force includes four components: the basal friction, the push force, the pull force, and the shearing forces. In fact, the push force, the pull force, and the shearing forces are all rooted from the basal frictions exerted by the asthenosphere along the bottom surface of related crusts. The basal friction involves in four factors, i.e., the asthenosphere's viscosity, the continent's area, the continent's speed, and the asthenosphere's thickness. Both the area and the speed can be exactly measured, but the viscosity and thickness of the asthenosphere remain high uncertainty according to different authors. Cathless (1971) concluded the viscosity no less than 10^{20} P, Jordan (1974) treated the thickness as 300 km. Fjeldskaar (1994) suggested that the asthenosphere has a thickness of less than 150 km and a viscosity of less than $7.0*10^{20}$ P. Some works using glacial isostatic adjustment and geoid studies concluded the asthenospheric viscosity ranges from 10^{19} to 10^{21} P (Hager and Richards, 1989; King, 1995; Mitrovica, 1996). James et al. (2009) used model to show that the asthenospheric viscosity is varied from $3*10^{19}$ P for a thin (140 km) asthenosphere to $4*10^{20}$ P for a thick (380 km) asthenosphere. These totally result in that the total resistive force cannot be exactly got. Our treatment, however, must be practically acceptable. The basal friction exerted by the asthenosphere along the continent's base may be expressed as $F_A=\mu Au/y$, where μ, A, u, and y are respectively the viscosity of the asthenosphere, the continent's area, the continent's speed, and the thickness of the asthenosphere. We here adapt $\mu= 3*10^{19}$ P and y=140 km to estimate the basal friction for the selected four continents (South American, African, Indian, and Australian). The speeds of these continents are valued as 2.7, 4.2, 5.6, and 6.4 cm/yr, respectively, and their areas are listed in Table 1. Table 2 shows the estimated results of the basal frictions. Evidently, for each of these continents the horizontal force generated in magnitude is extremely close to the basal friction. We believe this approach is not coincidence, because these two kinds of forces are got through two different passages. Such an approach suggests that the treatment above may be acceptable.

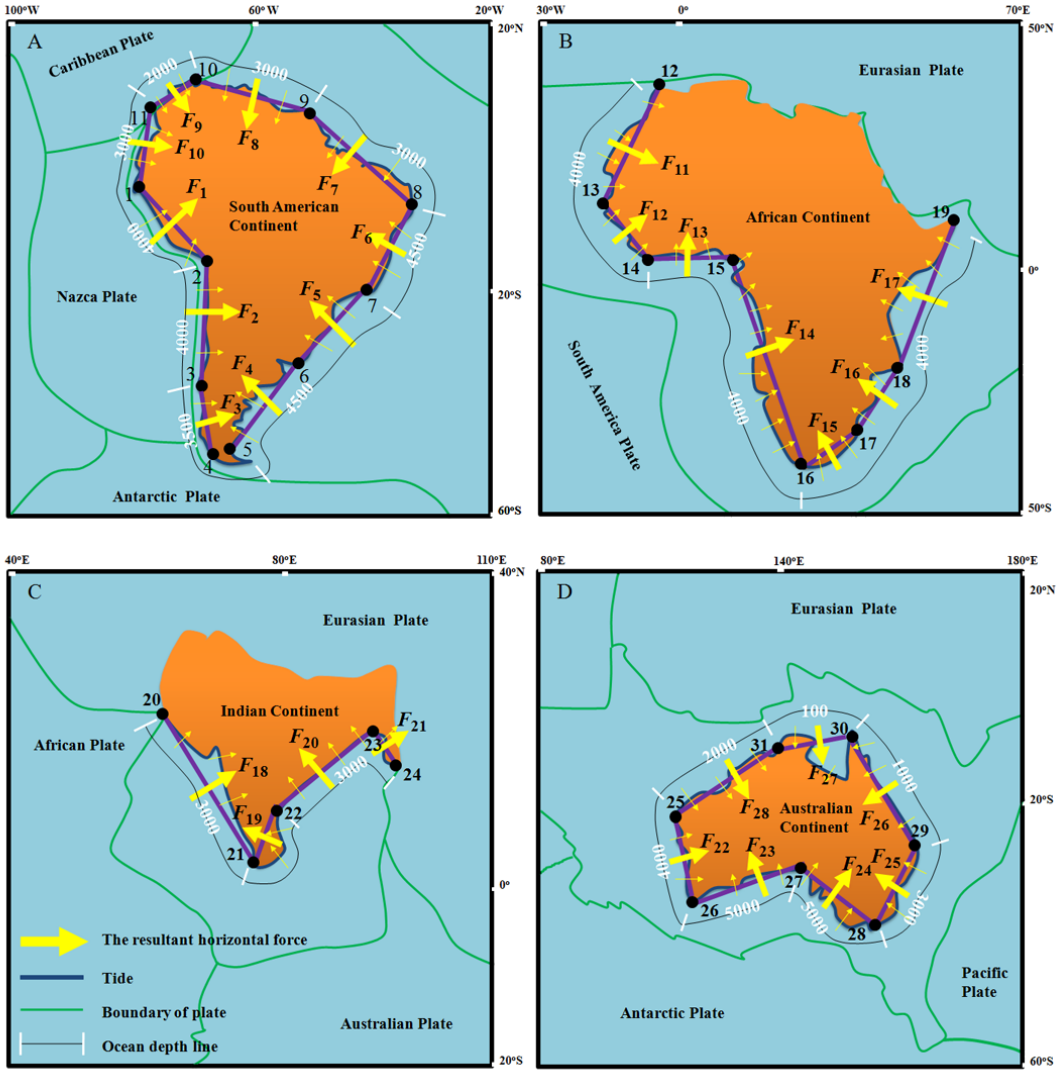

Fig. 5. Geographic treatment of the controlling sites for selected continents and the resultant horizontal forces exerted on them. *F* (yellow arrow) denotes the horizontal force generated, while purple bar denotes the distance applied by the horizontal force. The product of this distance and ocean depth is the area applied by the horizontal force. Dot with number denote controlling site. Ocean depth is artificially resolved from Google Earth software.

Table 1 Basic information for selected four continents

Continent	area	thickness	density	mass	site			site to site				tide amplitude	ocean depth
								distance		inclination to latitude, east (+)			
	S	d	ρ	M				L		i	Ω_i	h_{tide}	h_{ocean}
	km^2	km	kg/m^3	kg	No.	Longitude	Latitude	km			degree (^{o})	m	m
South American	17,840,000	6	3,100	3.32E+20	1	80.0^{o}W	2.0^{o}S	1_2	2,087	1	122.01	1.5	4,000
					2	70.0^{o}W	18.0^{o}S	2_3	1,153	2	73.30	1.5	4,000
					3	73.0^{o}W	28.0^{o}S	3_4	2,780	3	90.00	1.5	3,500
					4	73.0^{o}W	53.0^{o}S	5_6	2,308	4	51.15	2.0	4,500
					5	68.0^{o}W	52.5^{o}S	6_7	1,730	5	43.78	2.0	4,500
					6	54.0^{o}W	34.5^{o}S	7_8	1,952	6	64.89	1.5	4,500
					7	42.0^{o}W	23.0^{o}S	8_9	2,525	7	146.66	1.5	3,000
					8	34.0^{o}W	7.0^{o}S	9_10	2,157	8	160.64	1.5	3,000
					9	53.0^{o}W	5.5^{o}N	10_11	836	9	41.26	1.5	2,000
					10	72.0^{o}W	12.0^{o}N	11_1	1,033	10	75.66	1.5	3,000
					11	78.0^{o}W	7.0^{o}N						
African	30,370,000	6	3,100	5.65E+20	12	6.0^{o}W	35.5^{o}N						
					13	17.0^{o}W	14.7^{o}N	12_13	2,535	11	117.65	1.0	4,000
					14	7.0^{o}W	4.6^{o}N	13_14	1,531	12	45.00	1.0	4,000
					15	8.0^{o}E	4.4^{o}N	14_15	1,696	13	3.81	1.0	4,000
					16	22.2^{o}E	34.7^{o}S	15_16	4,577	14	109.75	1.0	4,000
					17	30.4^{o}E	30.7^{o}S	16_17	886	15	26.00	1.0	4,000
					18	40.0^{o}E	16.0^{o}S	17_18	1,904	16	56.85	1.0	4,000
					19	51.0^{o}E	11.0^{o}N	18_19	3,237	17	67.83	1.0	4,000
Indian	4,400,000	6	3,100	8.18E+19	20	66.8^{o}E	25.0^{o}N						
					21	77.5^{o}E	8.0^{o}N	20_21	2,205	18	122.19	2.0	3,000
					22	80.0^{o}E	15.2^{o}N	21_22	846	19	70.85	2.0	3,000
					23	91.5^{o}E	22.7^{o}N	22_23	1,468	20	33.11	2.0	3,000
					24	94.3^{o}E	16.0^{o}N	23_24	801	21	112.68	2.0	3,000

					25	114.0°E	23.0°S	25_31	2,162	28	32.43	2.0	2,000
					26	117.2°E	35.0°S	25_26	1,370	22	104.93	2.0	4,000
					27	131.0°E	31.5°S	26_27	1,340	23	14.23	1.0	5,000
Australian	8,600,000	6	3,100	1.60E+20	28	149.8°E	37.6°S	27_28	1,846	24	162.02	1.0	5,000
					29	153.0°E	25.4°S	28_29	1,390	25	75.30	2.0	3,000
					30	142.4°E	10.8°S	29_30	1,970	26	125.98	2.0	1,000
					31	131.0°E	12.2°S	30_31	1,252	27	7.00	2.0	100

Note: all geographic sites refer to Figure 5; tide amplitude is half of tidal range.

Table2 The resultant horizontal force and constrained resistive force for selected four continents

Continent	the horizontal force [a]									the total resistive force [b]	the basal friction[c]
	F_{ocean}					F_{tide}					
	i	horizontal	decomposed: latitudinal , east (+)	decomposed: longitudinal , north(+)	composition	i	horizontal	decomposed: latitudinal , east (+)	decomposed: longitudinal , north(+)	composition	$F_{resistive}$	f_{base}
		$F_{i\text{-}ocean}$	$F_{i\text{-}ocean\text{-}latitudinal}$	$F_{i\text{-}ocean\text{-}latitudinal}$			$F_{i\text{-}tide}$	$F_{i\text{-}tide\text{-}latitudinal}$	$F_{i\text{-}tide\text{-}latitudinal}$			
		N (*10^{17})					N (*10^{14})				N (*10^{17})	
South American	1	1.6362	1.3875	0.8672		1	1.2274	1.0408	0.6505			
	2	0.9043	0.8661	-0.2598		2	0.6783	0.6497	-0.1949			
	3	1.6686	1.6686	0.0000		3	1.4306	1.4306	0.0000			
	4	2.2905	-1.7837	1.4369		4	2.0364	-1.5859	1.2775			
	5	1.7169	-1.1879	1.2395		5	1.5264	-1.0561	1.1021			
	6	1.9365	-1.7535	0.8219		6	1.2912	-1.1692	0.5480			
	7	1.1136	-0.6121	-0.9304		7	1.1139	-0.6122	-0.9306			
	8	0.9510	-0.3153	-0.8973		8	0.9513	-0.3153	-0.8975			
	9	0.1639	0.1081	-0.1232		9	0.2460	0.1622	-0.1849			
	10	0.4555	0.4413	-0.1128		10	0.4556	0.4414	-0.1128			
			-1.1807	2.0421	2.3588			-1.0140	1.2574	1.6153	2.3604	3.2730
African	11	1.9873	1.7604	-0.9221		11	0.9938	0.8803	-0.4611			
	12	1.2000	0.8485	0.8485		12	0.6001	0.4243	0.4243			

	13	1.3298	0.0885	1.3268		13	0.6650	0.0442	0.6635			
	14	3.5882	3.3772	1.2123		14	1.7943	1.6888	0.6062			
	15	0.6949	-0.3047	0.6246		15	0.3475	-0.1524	0.3123			
	16	1.4924	-1.2496	0.8160		16	0.7463	-0.6249	0.4081			
	17	2.5379	-2.3503	0.9575		17	1.2691	-1.1753	0.4788			
			2.1700	4.8637	5.3259			1.0851	2.4322	2.6633	5.3283	8.6672
Indian	18	0.9724	0.8230	0.5180		18	1.2970	1.0977	0.6909			
	19	0.3729	-0.3523	0.1223		19	0.4974	-0.4699	0.1631			
	20	0.6474	-0.3536	0.5422		20	0.8634	-0.4717	0.7232			
	21	0.3531	0.3258	0.1362		21	0.4710	0.4346	0.1816			
			0.4429	1.3187	1.3911			0.5907	1.7589	1.8554	1.3929	1.6743
Australian	22	1.0740	1.0377	0.2767		22	1.0743	1.0380	0.2768			
	23	1.6411	-0.4034	1.5907		23	0.6565	-0.1614	0.6363			
	24	2.2618	0.6981	2.1514		24	0.9048	0.2793	0.8607			
	25	0.6129	-0.5929	0.1555		25	0.8175	-0.7907	0.2074			
	26	0.0965	-0.0781	-0.0567		26	0.3865	-0.3128	-0.2271			
	27	0.0006	0.0001	-0.0006		27	0.0248	0.0030	-0.0246			
	28	0.4237	0.2272	-0.3577		28	0.8479	0.4547	-0.7157			
			0.8887	3.7594	3.8630			0.5100	1.0138	1.1349	3.8640	3.6815

Note: all related forces refer to Figure 5.
a (the horizontal force) and *c* (the basal friction) are calculated, while *b* (the total resistive force) is valued.

Table 3 The resultant movements for selected four continents

Continent	movement per year	to latitudinal direction, east (+)
	mm/yr	degree
South American	27.59	120.04
African	41.85	65.96
Indian	56.46	71.44
Australian	63.09	76.70

The treatments on the continent's movement above are reliable only for these small-sized continents. For those larger ones like Eurasian and North American continents, as their curvatures cannot be ignored, the horizontal forces generated cannot pass their barycenters, a torque effect may be yielded to rotate them. Figure 6 (A and B) conceptually demonstrates how these continents move under the torque effect of the resultantly horizontal forces.

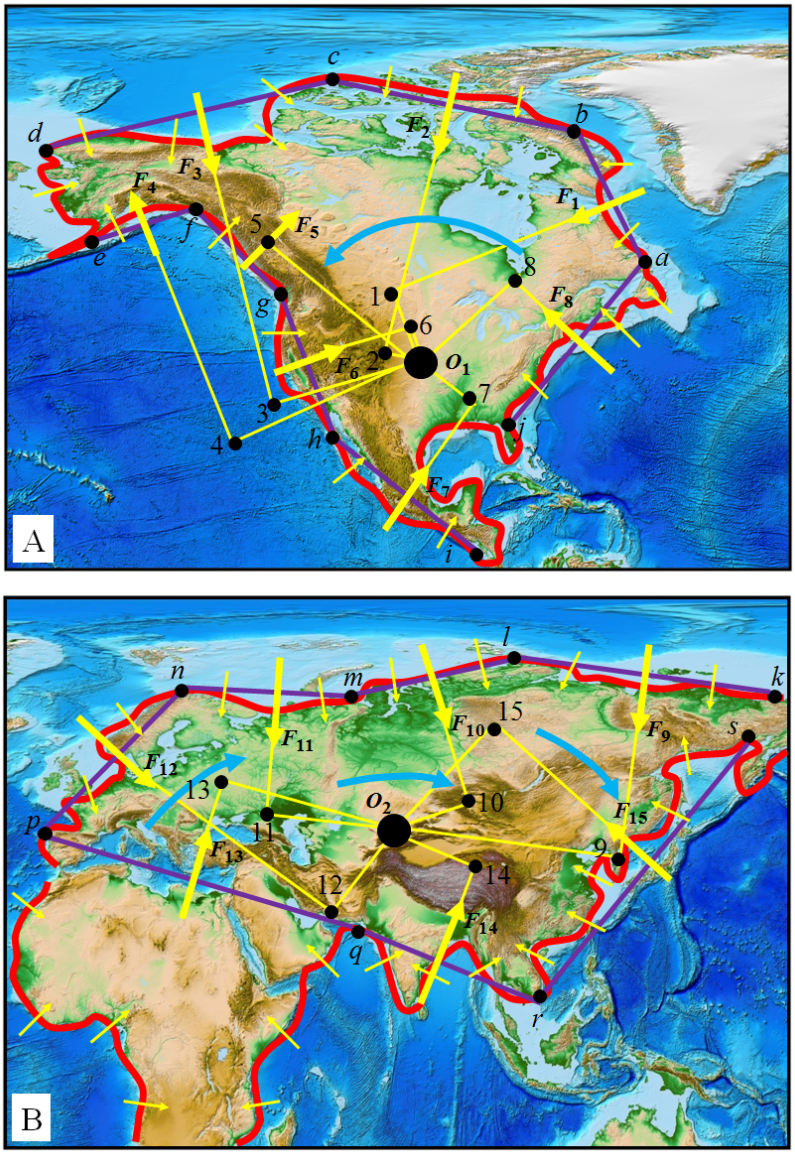

Fig. 6. Dynamics for the rotations of North American and Eurasian continents. O_1 and O_2 denote possible positions of the barycenters of two continents. F_1, F_2, F_3, i.e., marked with yellow arrows, denote the horizontal forces yielded, *a*, *b*, *c*, i.e., denote the selected controlling sites, while *ab*, *bc*, *cd*, i.e., marked with purple bars, denote the length of continent's side, while $O_1$1,

O_12, . . ., O_29, O_210, i.e., denote the arms applied by the horizontal forces. Torque effect is expressed with a product of force and arm. Curved blue arrows represent some expected rotations around these barycenters. Note F_{13} represents a lateral push force from the travelling African continent. The background map is got from ETOPO1 Global Relief Model (Amante and Eakins, 2009).

2.3 Plate motion

Plate motion may be a result of the ocean-generating force. As shown in Figure 1 and Table 2, a majority of the net horizontal force generated is used to oppose the total resistive force, which consists of the basal friction exerted by the asthenosphere, the push force from the crust at the right side, the pull force from the crust at the left side, the shearing force from the crust at the far side, and the shearing force from the crust at the near side. By the principle of action and reaction, these forces further drive the crusts that bear them to move, it is such an interactive process to create plate motion over the globe.

Force transferring from one plate to another can be represented with Pacific Plate's motion. As outlined in Figure 7, the northeasterly travelling Australian Plate and the rotating North American Plate independently provide push force F_{PA} and F_{PN} to Pacific Plate, a composition of these two forces would be the force F_{P}, which provides a dynamics for Pacific Plate. Quantifying Pacific Plate's motion is somewhat complicated. At first, it is assumed that Pacific Plate is more rigid and planar. This allows plate deformation to be negligible. According to a relationship of movement and force, the equation (2) may be simplified as $F \sim DM$, where F is the net force that a continent accepts, M is the continent's mass, and D is the resultant movement. Applying this simplified relationship to South American continent, it would be $F_S \sim D_S M_S$. Furthermore, we apply this relationship to North American continent and make analogy with South American continent, there would be $F_N \sim F_S D_N M_N / D_S M_S$, where F_N and F_S denote the net horizontal force accepted respectively by North American continent and by South American continent, D_N and D_S denote the resultant movement respectively for them,

and M_N and M_S denote the masses of these continents. Refer to the parameters listed in Table 1, 2, and 3, there would be F_S=2.3605*10^{17} N, D_S=2.7 cm per year, M_S=3.32*10^{20} kg. North American continent holds an area of about 24,709,000 km^2, according to an expression $M=Sd\rho_{continent}$ (where S, d, and $\rho_{continent}$ are respectively the continent's area, thickness, and density), the continent's mass is figured out to be M_N=4.60*10^{20} kg. North American Plate (continent) rotates counter clockwise and moves with a speed of about 1.5~2.5 cm per year, we adapt D_N=2.0 cm per year for the western portion of this plate to interact with Pacific Plate. And then, the net horizontal force calculated for North American continent should be F_N =~2.4227*10^{17} N. To operate North American Pate, the net horizontal force F_N needs to overcome the total resistive force that this continent bears, which consists of mainly the push force from Pacific Plate and the shearing force from South American Plate. As the push force and the shearing force are all related to the basal friction exerted by the asthenosphere, and further refer to the basal friction expression $F_A=\mu Au/y$, it would be F_A~A, the push force from Pacific Plate may be linearly written as $F_{PN}= F_N S_P/(S_P+S_N)$=1.0261*$10^{17}$ N, where S_P and S_N are respectively the area of Pacific Plate and South American Plate. Refer to table 2, the total resistive force for Australian plate is $F_{Au\text{-}resistive}$ =3.8640*10^{17} N, we assume that about 25% of this force is used to oppose the push force from Pacific Plate, and then, the push force is worked out to be F_{PA}=9.6600*10^{16} N. By the principle of action and reaction, Pacific Plate finally obtains one push force F_{PN} from North American Plate and another push force F_{PA} from Australian Plate. Australian Plate moves dominantly in a northeast direction that is inclined to latitude, the angle between this direction and latitude is about 76.7°, as shown in Table 3. Most of North American Plate, however, moves roughly in a southwest direction away from the Mid-Atlantic Ridge, we adapt the push force from the part of North American Plate, which contacts Pacific Plate, to be arranged in a southwest direction, the angle between this direction and latitude is about 190°. The net horizontal force accepted by Pacific Plate may then be $F_P=((F_{PN}^2+F_{PA}^2-2*F_{PN}F_{PA}*\cos(\alpha-\beta))^{0.5}$, and $\cos\gamma=(F_P^2+F_{PN}^2-F_{PA}^2)/(2*F_P*F_{PN})$, where α=76.7°, β=10°. Finally, it is worked out to be F_P=1.096315*10^{17} N, and γ=54.03°. Similarly, we assume that a majority of the net horizontal force accepted by Pacific Plate has

been used to oppose the total resistive force, which consists of mainly the friction exerted by the asthenosphere along Pacific Plate's base. Refer to Table 2, the ratio between the total resistive force and the net horizontal force for South American continent may reach up to 0.99999907. Compared to this ratio, it is allowable to consider a ratio of 0.99999 for Pacific Plate, and then, the total resistive force for Pacific Plate will be $F_{Pa\text{-}resistive}$=1.096304*10^{17} N. Refer to Table 1, the continent's thickness is valued as 6.0 km, the average ocean depth is less than 4.0 km, this allows a thickness of 2.0 km to be left for the continental crust to contact the oceanic crust. Pacific Plate's mass may be expressed as $M_{\text{Pacific}}=S\text{d}\rho_{\text{plate}}$ (where S, d, and ρ_{plate} are respectively the plate's area, thickness, and density). If we assume the plate's density to be equal to the continent's density, and adapt Pacific Plate's area to be 103,300,000.00 km^2, and then, there would be M_{Pacific}= 6.4046*10^{20} kg. The equation (2) may be further simplified as $D \approx 365*2*(0.5*(F_{ocean}+F_{\text{max-}tide}-F_{resistive})*t^2/M)$, where $(F_{ocean}+F_{\text{max-}tide})$ denotes the maximum net horizontal force that the continent accepts, $F_{resistive}$ denotes the total resistive force that the continent accepts. According to the equation (3) and refer to Table 2, the time that Australian continent takes to accelerate during a tide is t=2*arccos(2($F_{resistive}$-F_{ocean})/$F_{\text{max-}tide}$-1)/3=378.35 s. Applying this simplified equation to resolve Pacific Plate's motion, it would be D=365*2*(0.5*(F_{P}-$F_{Pa\text{-}resistive}$)*t^2/M_{Pacific})=89.44 mm per year, a roughly northwest direction, the angle between this direction and latitude is 44.03^{o}.

Nevertheless, if we look at North American Plate from a viewpoint of evolution, it must had rotated too much during a timescale of more than millions of years, this means that North American Plate could be oriented towards northeast in the past, if so, the push force F_{PN} may be not existed at that time, subsequently, Pacific Plate was most likely pushed by Australian Plate alone to move along northeast. This means that, an abrupt change in motion might had occurred for Pacific Plate at a time when North American Plate rotated to a central angle, from where a combination of the two lateral forces considered above becomes possible. Such a plate motion change has been actually witnessed by the Hawaiian–Emperor bend (Sharp and Clague, 2006; Wessel and Kroenke, 2008).

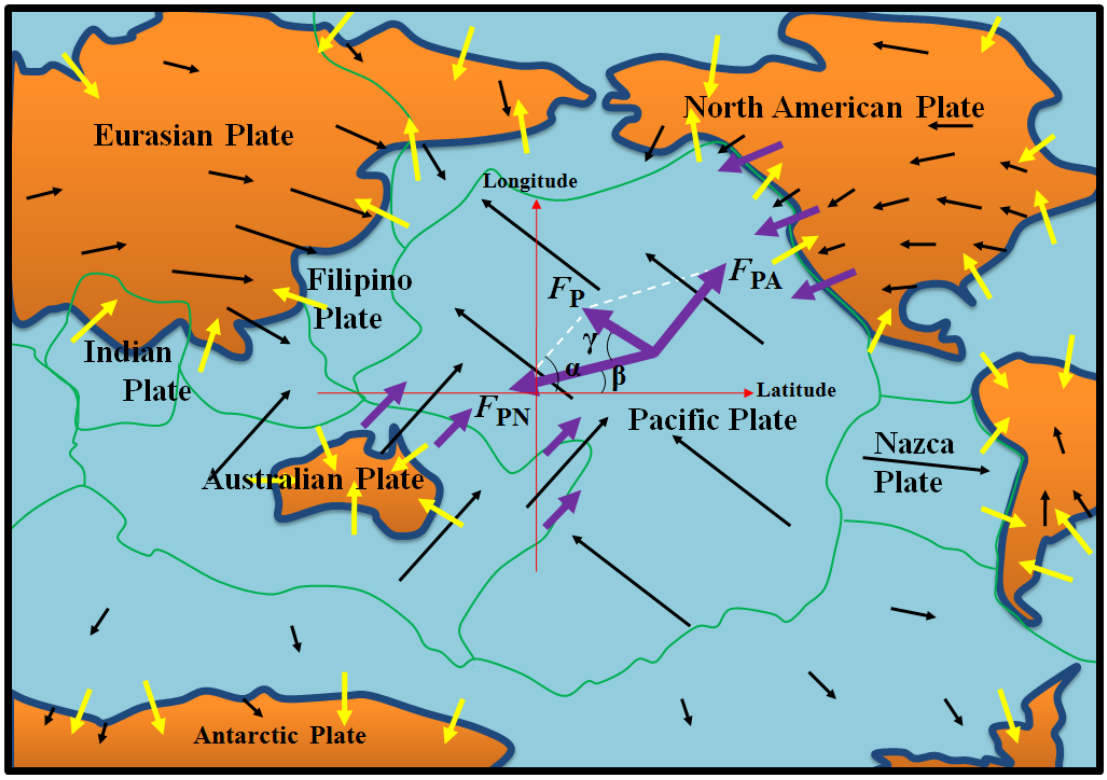

Fig. 7. Modelling the dynamics of Pacific Plate. Black, yellow, and purple arrows denote respectively plate motions, the resultant horizontally forces, and lateral push forces from related plates. Note lateral push force F_{PN}(F_{PA}) is approximately parallel to the motion of North American (Australian) Plate.

3 Discussion

3.1 Comparison of the ocean-generating force and ridge push force

As shown in Figure 4, the ocean-generating forces exert generally orthogonal to the continents' coastlines, and the shapes of the ridges trend to follow that of these coastlines. This final point is particularly correct for the continental plates like North American, South American, Africa, and Indian-Australian. Ridge push forces (if existed) exert generally orthogonal to the ridges. This fitting of direction means that, if we use torque analysis to determine, these two forces cannot be distinguished. Nevertheless, they are different in both the position of force acting on plate and the distribution of compression (Figure 8). For example, the ocean-generating forces (F_o) exert on the upper part of plate 2, while ridge push

force (F_p) exerts on the middle and lower part of this plate. These two kinds of forces can all result in horizontal compressions on the plate. Geometrically, the compression generated due to the former would cross the upper part of the plate, while the compression generated due to the latter would cross the middle and lower part of the plate.

Tectonic stresses are caused by the forces that drive plate tectonics (Middleton and Wilcock, 1996). Thus, tectonic stresses may provide feedback on the constrain of the forces acting on the plates. Tectonic stress measurements had discovered remarkable features on the global patterns of tectonic stress (Zoback et al., 1989; Zoback, 1992): (1) The interior portions of plates (also called midplate or intraplate) are dominated by compression in which the maximum principal stress is horizontal. (2) In most places a uniform stress field exists throughout the upper brittle crust. (3) A strong correlation between S_{Hmax} (maximum horizontal stress) orientations and azimuths of absolute plate velocity exists in the interior portions of some plates. Additionally, detailed analysis of stress measurement data show that S_{Hmax} orientations are often rotated into a plane approximately parallel to the local trend of the continental slope. It is very striking to see, these patterns of tectonic stress trend to favor a force that is closely related to continent. For most of plates like North American and South American, their interiors are mainly covered with continents. In particular, the tectonic stress measurements were concentrated on continents (Zoback et al.,1989). According to Zoback (1992), these measurement data came from four passages: earthquake focal mechanisms, well bore breakouts, in situ stress measurements (hydraulic fracturing and overcoring), and young geologic data including fault slip and volcanic alignments. Of these, the most reliable are well bore breakouts and in situ stress measurements. These two operated in a depth of generally less than 5.0 km. This shallower region is almost dominated by continent. Moreover, the correlation between S_{Hmax} orientations and the continental slope is an indicator of such a force. Undoubtedly, the best candidate for this force is the ocean-generating force.

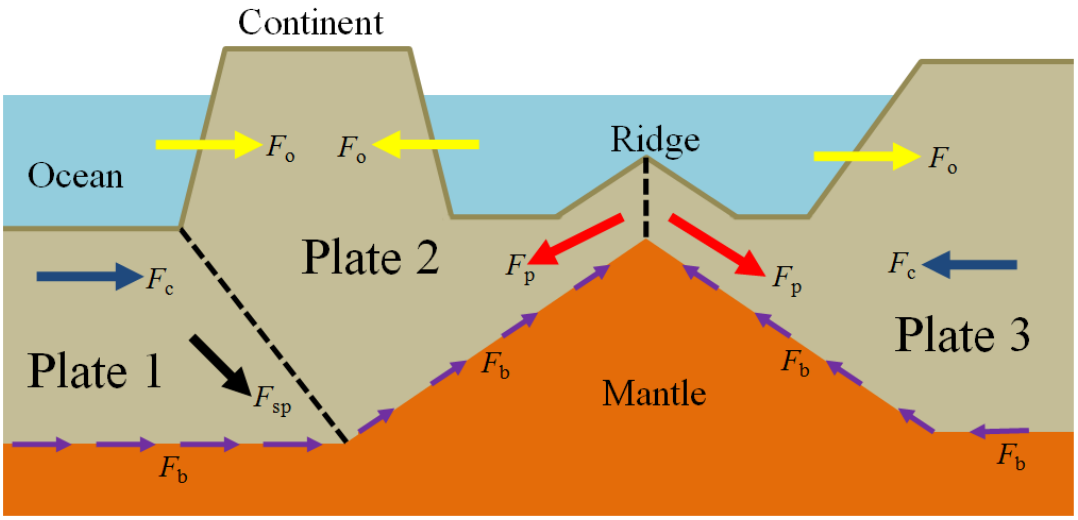

Fig. 8. Comparison of the ocean-generating force and the established driving forces. F_o, F_p, F_c, F_{sp}, and F_b denote respectively the ocean-generating force, ridge push force, collisonal resistence, slab pull, and basal drag. Note that the direction of basal drag is determined based on the assumption that plate 2 moves towards left.

Some authors employed a comparison of magnitude between the ocean-generating force and ridge push force to conclude that the ocean-generating force is insignificant. We here provide two points to argue. On the one hand, such a comparison itself is meaningless. The large uncertainties of ridge push force that are exposed in section 1 make the comparison become useless. In addition, the Newton's 2nd law shows that an object's movement is determined by both the magnitude of force and the time that the force works on the object. The magnitude is just one of the two factors. On the other hand, even if we assumed ridge push force to be valid, it is still unclear whether it is greater than the ocean-generating force or not. According to these authors (McKenzie, 1972; Forsyth & Uyeda,1975), ridge push force was expressed as $F = \Delta PlL = g(\rho_0-\rho_w)elL/2$, where l and L are the thickness of the lithosphere and the length of the ridge, ΔP is the mean excess pressure and can be further written as $\Delta P = g(\rho_0-\rho_w)e/2$ (where e is the elevation of the ridge above the deep sea floor and ρ_0 and ρ_w are the densities of the lithosphere and sea water, respectively). Given e=3,000 m, l=100 km, L=1.0 m, ρ_0=3,000 kg/m^3, ρ_w=1,000 kg/m^3, and g=10 m/s^2, this expression results in a ridge push force of

magnitude $3*10^{12}$ N. This estimation, however, is seriously flawed. As mentioned earlier, the application of liquid pressure over the entire side of a vessel yields lateral force. The core of this physics is that liquid particles freely strike the vessel's side to form a forcing effect, i.e., lateral force. We believe, in a vessel the viscosity of liquid plays an important role in determining this lateral force. For example, the viscosity of water at temperature 20° is 1.0 mPas, this low viscosity allows water particles to freely strike the side of a vessel that holds them. This property of molecular movement makes scientific community accept that the pressure exerted by liquid over the entire side of a vessel may be expressed as $P=\rho g h/2$, which is just half of the pressure exerted by liquid on the bottom of that vessel, where ρ and h are liquid's density and depth. The viscosity of tar at temperature 20° is 30,000 Pas, such a high viscosity would largely restrict tar particles to strike the side of the vessel that hold them, therefore, the pressure exerted by tar over the entire side of a vessel may be far less than half of the pressure exerted by them on the bottom of that vessel. Practically, the MOR's beneath is filled with asthenospheric materials. The viscosity of these materials ranges from 10^{18} to 10^{20} Pas (Hager and Richards, 1989; King, 1995; Mitrovica, 1996). Such an extreme high viscosity makes these materials more like solid than liquid. Finally, the expression of ridge push force (i.e., $F = \Delta PlL = g(\rho_0-\rho_w)elL/2$) above and its resultant result (a ridge push force of magnitude $3*10^{12}$ N) cannot be valid. In contrast, the ocean-generating force presented here may be expressed as $F = g\rho_w l^2 L/2$, where l and L are respectively the depth and length of ocean water. Given a water depth of 5,000 m and a water length of 1.0 m, this expression results in a force of magnitude $1.25*10^{11}$ N. Such a magnitude, as demonstrated in section 2, is competent for yielding the requisite plate motion.

3.2 Clarification on tidal drag driving mechanism

Tidal drag proposed as a driving mechanism for plate motion had been long debated. Wegener (1924) attributed the westward drift of the American blocks to tidal drag, but Jeffreys (1929) argued that the westward stress related to tidal drag is too small to be competent for the displacement. A rapid growth of tidal drag driving mechanism arises from the confirmation of

a net rotation or westward drift of the lithosphere relative to the mantle (Rittmann, 1942; Le Pichon, 1968; Bostrom, 1971; Moore, 1973), which is supported by independent observations such as plate motion within the hot spot reference frame (Ricard et al., 1991; O'Connell et al., 1991; Gordon, 1995; Gripp and Gordon, 2002), plate motion relative to Antarctica (Le Pichon, 1968; Knopoff and Leeds, 1972), and supported by geological asymmetries (Doglioni, 1993). Another supporting to it comes from energy budget. For instance, many works showed that tidal drag is energetically feasible for plate motion. According to Rochester (1973) and Jordan (1974), the total energy released due to tidal friction exceeds $5*10^{19}$ ergs/s, excluding the dissipation in both shallow seas and solid Earth (Miller, 1966; Munk, 1968), a remaining energy of about $3*10^{19}$ ergs/s might be available for driving plate motion, this amount exceeds by 2 orders of magnitude the lower bound set by seismic energy release (Gutenberg, 1956). Some authors (Egbert and Ray, 2000; Ray, 2001; Riguzzi et al., 2010) recently reevaluated the energy budget to show that the total energy released by tidal friction may reach up to $1.2*10^{20}$J/yr, subtracting the dissipation in the mantle, oceans, and shallow seas, a residual energy of about $0.4*10^{20}$J/yr is larger than the one required to maintain the net rotation, estimated at about $1.27*10^{19}$J/yr. Nevertheless, a satisfaction in energy supply cannot shield tidal drag driving mechanism. Both Jordan (1974) and Jeffreys (1975) showed that the viscosity both related to tidal drag and necessary to allow decoupling between lithosphere and mantle ($\sim 10^{11}$ Pas) is far less than the present-day asthenosphere viscosity, estimated at between 10^{17} and 10^{20} Pas (Anderson, 1989; Pollitz et al., 1998; Fjeldskaar, 1994; Giunchi et al., 1997; Piersanti, 1999). Ranalli (2000) further showed that any non-zero torque due to difference in angular velocity between the mantle shell and lithosphere shell would be extremely transient, and therefore cannot be a factor in the origin of the westward drift of the lithosphere. In spite of these arguments, tidal drag driving mechanism continues to grow up. Scoppola et al. (2006) proposed the westward rotation of the lithosphere as the consequence of a combined effect of tidal torque acting on the lithosphere, downwelling of the denser material toward the deeper interior of the Earth, and thin layers of very low viscosity hydrate channels occurring in the asthenosphere. A few authors recently showed that, by assuming an

ultra-low viscosity layer in the upper asthenosphere, the horizontal component of the tidal oscillation and torque have ability to move the lithosphere (Riguzzi et al., 2010; Doglioni and Panza, 2015).

If we compare the tidal drag with the ocean-generating force, a few points may be extracted to share: First of all, the tidal drag is proposed to explain the westward drift of the lithosphere relative to the mantle, while the ocean-generating force is proposed to explain the various plate motions; Secondly, the tidal drag has no objection to the established plate driving forces, and therefore, it may be the supplementary to these forces. In contrast, the ocean-generating force may be independently responsible for plate motion, and therefore, it is the primary plate driving force. We believe, if these established driving forces can be proven further, they may be the supplementary to the ocean-generating force; Lastly, as shown in Table 2, the horizontal force generated due to tide is less than 3 orders of the magnitude of the basal friction generated due to the asthenosphere, this point agrees to the conclusion made by Jordan (1974). However, the tide's significance mayn't be ignored. As inferred from Figure 3 and seen in Table 2, there is a balance between the ocean-generating force (i.e., $F_{\text{ocean}}+F_{\text{tide}}$) and the resistive force ($F_{\text{resistive}}$). The oscillation of ocean due to the addition of tide makes this balance periodically broken, by which a discontinuous net force is generated for the continent, finally, the continent obtains a steadily forward movement.

3.3 Extension of the continent's movement

The travelling continent drags the oceanic crust it connects in the rear, this pull yields strain for the oceanic crust. We believe, a periodically fracture of the oceanic crust might have been responsible for the formation of MOR. For example, as outlined in Figure 9, the continent continues to move, the accumulated strain eventually rip the oceanic crust, this fracture allows magma to erupt. The erupted magma after cooling crystallizes and creates new crusts. The newly formed crusts may help to seal the fracture and terminate the eruption. The fracture temporarily relieves the accumulated strain, but because the continent continues to move, the

strain is again accumulated, the following fracture and closeness occur again. The newly formed crusts add height to the oceanic crust, forming the MOR. The representative of this type of MOR is the Middle-Atlantic Ridge. Of course, not all the MORs are made through this way. For example, the travelling continent also shears the oceanic crusts at the far and near sides, these actions also may cause these crusts to fracture to form the MORs.

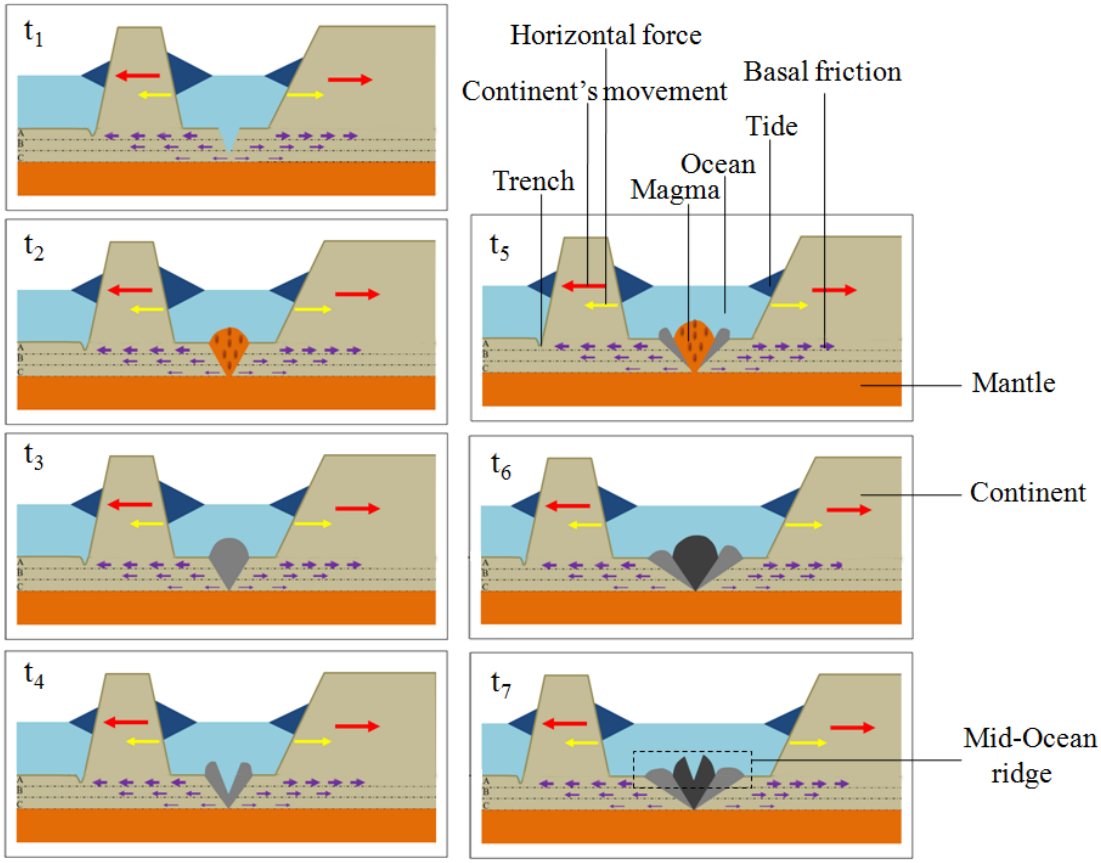

Fig. 9. Modelling the formation of MOR under the ocean-generating forces. From t_1, t_2, …, to t_7, it exhibits a sequence of forming the MOR. The lower lithosphere is apparently divided into three layers A, B, and C, so as to depict different motions due to the drag exerted by basal friction.

The travelling continent, if meet another continent in the front, would create high mountain. For example, refer to Figure 10, the horizontal force generated pushes Indian continent to impinge into Eurasian continent, as this force is almost vertical to the continental slope, this provides a bulldozer effect to uplift the materials in the front, forming the Himalayas. It is important to note that, the Himalayas was long ascribed to a result of the collision of Indian

Plate and Eurasian Plate. This understanding, however, is not exactly correct. The two plates have same rock density, the collision between them would result in an addition of height. The thickness of the continental (oceanic) crust is about 35 (6) km (Turcotte & Schubert 2002), an overlay of these two plates would yield a thickness of at least 70 km, in spite of the folded situation generated due to plate itself. Unfortunately, the present-day Himalayas (Mount Everest, 8,848 m) is still too low to match the requisite height. In contrast, if we ascribe the Himalayas to be a result of the collision of these two continents, it seems to be practicable. Both the Arabian Sea and Bay of Bengal hold a depth of about 4,000 m, it is this depth to bear the ocean-generating force. Indian continent holds a height of no more 500 m, Tibetan Plateau holds a height of about 4,000~5,000 m, if we add a continent of thickness 4,000 m, which is equal to the sea depth that yields the force, onto Tibetan Plateau, the requisite height may be got. Actually, the Himalayas provides a good example for us to understand the formation of the Alps. The Alps could arise from a collision of the travelling Italian island and Europe. A major reason for this consideration is the relatively deeper Ionian and Tyrrhenian seas provide a dominantly lateral push to Italian island. Of course, not all the mountains are made through this way. For instance, all continents are circled by oceans, the horizontal forces generated would push all the sides of a continent inwards, these actions deform the continent to create folded mountains.

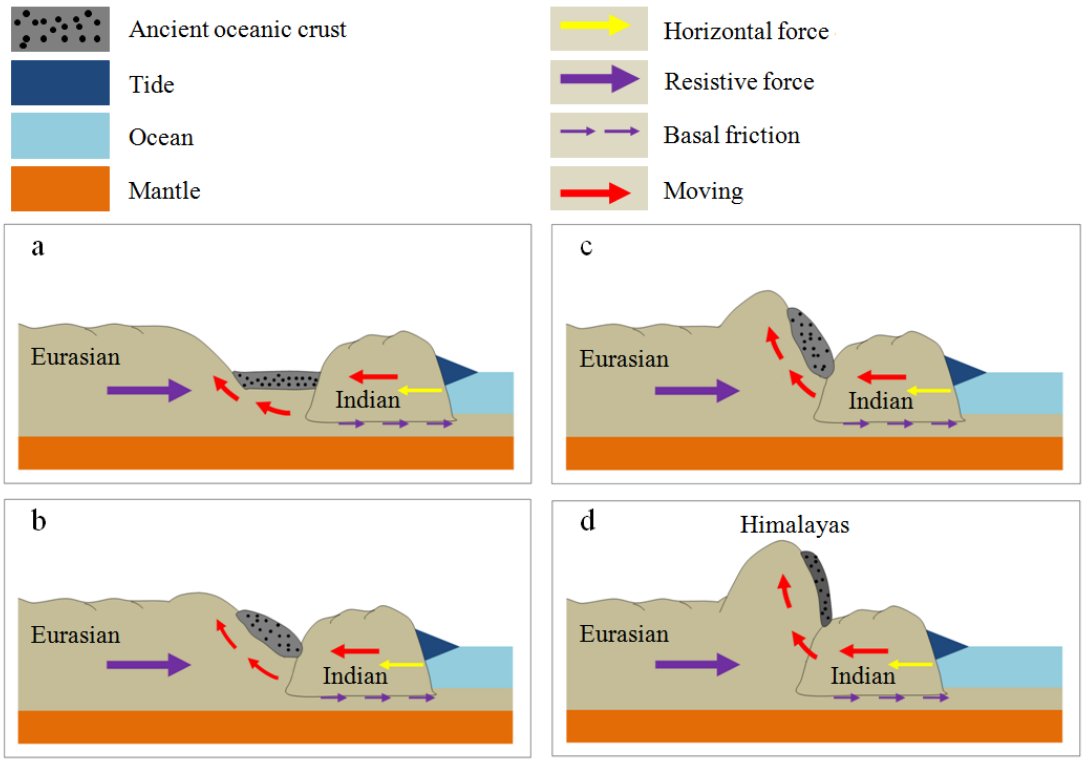

Fig. 10. Modelling the formation of the Himalayas under the collision of Indian continent and Eurasian continent. From a, b, …, to d, it shows a sequence of forming the mountain.

One of the most unusual features around the MOR is the transform faults which cut the ridge into a train of smaller sections, but the formation of these structures remains in a state of debate among scientific community (Gerya, 2012). The currently accepted view believes that the oceanic transform faults originated from plate fragmentation that is related to pre-existing structures (Wilson, 1965; Oldenburg and Brune, 1972; Cochran and Martinez, 1988; McClay and Khalil, 1998; Choi et at., 2008). Gerya (2010) recently theorized the transform fault of Mid-Atlantic Ridge. A distinguishable feature for the transform faults is there are many long and nearly-parallel structures that usually cross the ridge to exert the cutting, this suggests that the formation of the ridge is possibly later than that of these structures. We consider a solution for the transform faults of the Mid-Atlantic Ridge. As exhibited in Figure 11, the early Atlantic was relatively narrow, the horizontal forces generated continued to push the continents at both sides to move away, the travelling continents further dragged the oceanic crust they connect, the accumulated strain firstly split the oceanic crust into smaller

nearly-parallel segments. This way of nearly-parallel fracture benefits from that the horizontal forces generated exert generally orthogonal to the coastlines that are curved, subsequently, a large number of radially distributed strains are determined across the oceanic crust. For each of these nearly-parallel segments, the leading drag to it is exerted along nearly opposed directions, the accumulated strain is mostly possible to fracture it in the middle. The fracture, as demonstrated above, may yield a ridge. Finally, a ridge is formed for a segment, a connection of the ridges of all these segments forms the transform faults of the Mid-Atlantic Ridge.

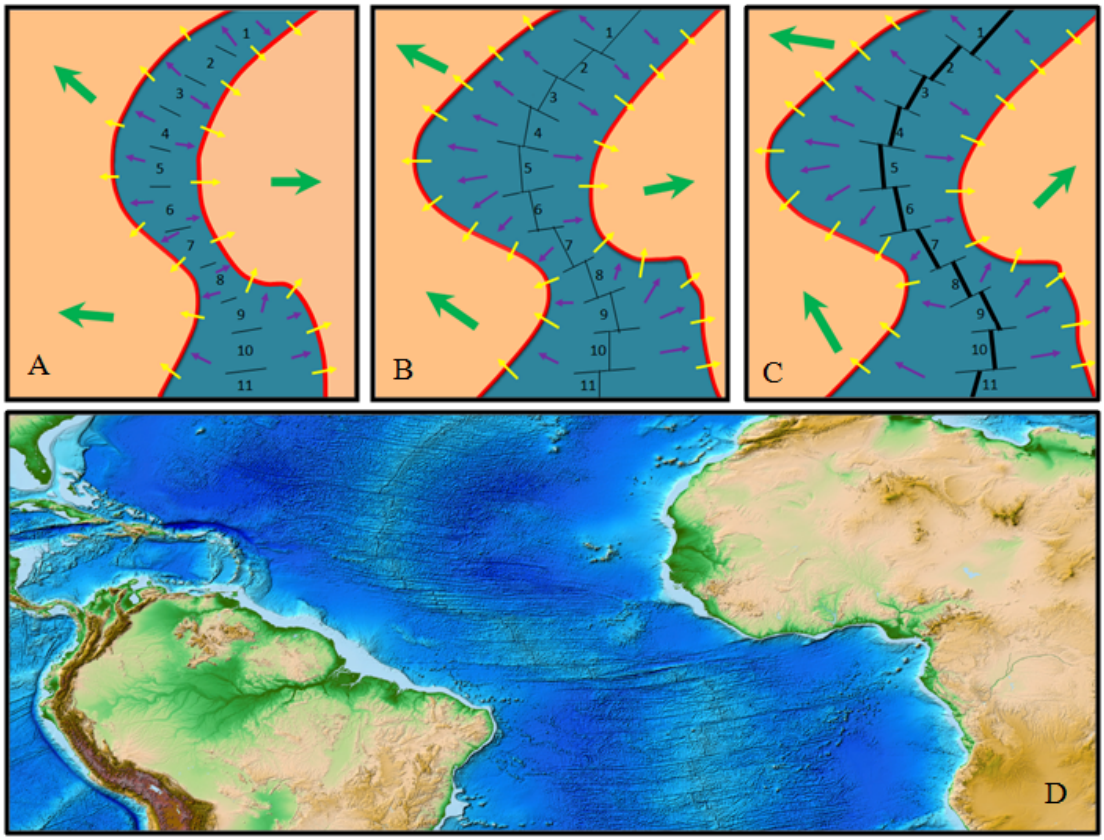

Fig. 11. Modelling the formation of MOR and transform faults. A, B, and C exhibit a sequence of how transform faults evolve with the growth of the MOR. Yellow, green, and purple arrows denote respectively the horizontal forces, the resultant movements, and the drags exerted by the travelling continents to the oceanic crust. The thin black lines represent nearly-parallel structures. Number 1, 2, . . ., and 11 represent the fragments of the oceanic crust, which consist of the section

of transform faults. D shows the transform faults over the Mid-Atlantic Ridge. The background map is produced from ETOPO1 Global Relief Model (Amante and Eakins, 2009).

The ocean-generating force driving mechanism provides line for us to conceptually track the dispersal of supercontinent. Refer to Figure 12, at the time of upper carboniferous the opening at the east of landmass at first allowed a large body of water to enter, the horizontal force generated pushed the landmass at the two sides of the opening to move away. This separation helped to expand the opening further. With the passage of time, the landmass was gradually separated and displayed the shape at the time of Eocene. This, again, facilitated more water to enter, and also more horizontal force to be generated. We speculate, such a positive feedback may have controlled the landmass's initial dispersal. The landmass was almost broken into pieces at the time of the older quaternary, a relatively primitive layout of separated smaller continents was formally established. After that, the horizontal force continued to push these continents to move away from each other until present.

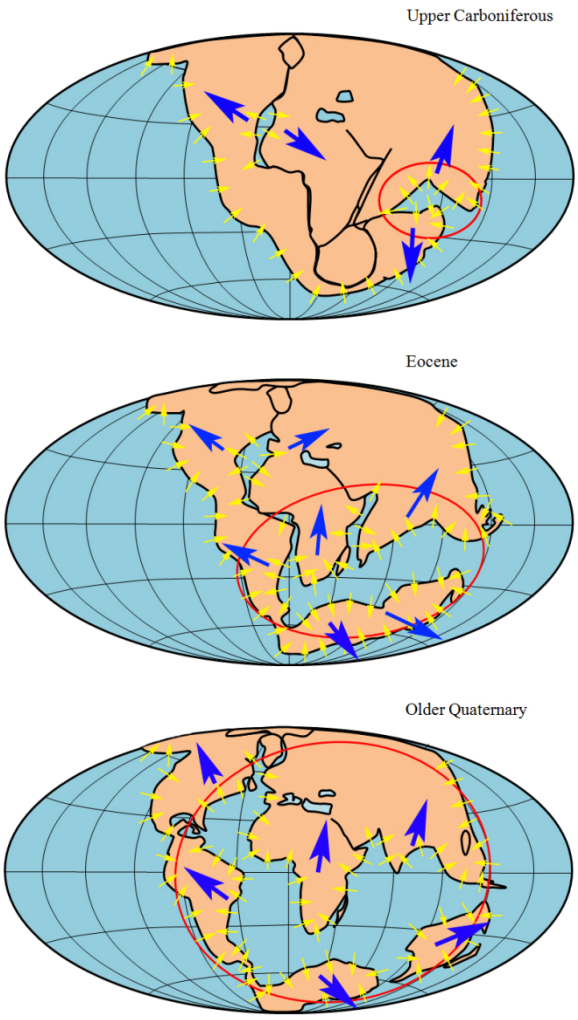

Fig. 12. Modeling the dispersal of supercontinent. Yellow and blue arrows denote respectively the horizontal forces and the resultant movements. Red circles represent an expansion of the ocean among the landmasses. The background map is yielded referring to Wegener's work (1924).

About 71% the Earth's surface is covered with the oceans of generally more than several kilometers in depth. Such a gigantic body of water makes people easy to think of a correlation between the ocean-generating force and the Earth's surface motion (i.e., plate motion). Many people feel extraordinarily perplexed why the Earth has plate tectonics but her twin Venus does not. A large number of works had addressed that water provides right conditions (maintaining a cool surface, for instance) for the Earth's plate tectonics, while the loss of water on the Venus prohibits plate formation (Hilairet et al., 2007; Korenaga, 2007; Lenardic

and Kaula, 1994; Tozer, 1985; Hirth and Kohlstedt, 1996; Lenardic et al., 2008; Landuyt and Bercovici, 2009; Driscoll and Bercovici, 2013). This work expands these understandings, no water on the Venus, no the ocean-generating force, naturally, no formation of plate tectonics on that planet.

Acknowledgments We express honest thanks to Maureen D. Long, Jeroen van Hunen, and Thorsten Becker for their suggestive comments.

References

Amante, C. and Eakins, B.W. (2009). ETOPO1 1 Arc-Minute Global Relief Model: Procedures, Data Sources and Analysis. NOAA Technical Memorandum NESDIS NGDC-24. National Geophysical Data Center, NOAA. doi:10.7289/V5C8276M.

Anderson, D.L. (1989). Theory of the Earth. InBlackwell, pp. 1-366.

Backus, G., Park, J. & Garbasz, D. (1981). On the relative importance of the driving forces of plate motion. Geophys. J. R. astr. Soc., 67,415-435.

Bercovici, D. (1993). A simple model of plate generation from mantle flow. Geophysical Journal International, 114, 635-650.

Bercovici, D. (1995b). A source-sink model of the generation of plate tectonics from non-Newtonian mantle flow. Journal of Geophysical Research, 100, 2013-2030.

Bercovici, D., Tackeley, P. J., and Ricard, Y. (2015). The generation of plate tectonics from mantle dynamics. Reference Module in Earth Systems and Environmental Science: Treatise on Geophysics (Second Edition), 7, 271-318.

Bokelmann, G. H. R. (2002). Which forces drive North America? Geology, 30(11), 1027-1030.

Bostrom, R. C. (1971). Westward displacement of the lithosphere. Nature, 234, 536-538.

Cadek, O., Ricard, Y., Martinec, Z., and Matyska, C. (1993). Comparison between Newtonian and non-Newtonian flow driven by internal loads. Geophysical Journal International, 112, 103-114.

Caldwell, P. C., Merrfield, M. A., Thompson, P. R. (2015). Sea level measured by tide gauges from global oceans — the Joint Archive for Sea Level holdings (NCEI Accession 0019568), Version 5.5, NOAA National Centers for Environmental Information, Dataset, doi:10.7289/V5V40S7W.

Cathies, L. (1971). The viscosity of the Earth's mantle, Ph.D. thesis, Princeton Univ., Princeton, N.J.

Choi, E., Lavier, L., Gurnis, M. (2008). Thermomechanics of mid-ocean ridge segmentation. Phys. Earth Planet. Inter., 171, 374-386.

Christensen, U., Harder, H. (1991). Three-dimensional convection with variable viscosity. Geophysical Journal International, 104, 213-226.

Cochran, J. R., Martinez, F. (1988). Evidence from the northern Red Sea on the transition from continental to oceanic rifting. Tectonophysics, 153, 25-53.

Conrad, C. P., Lithgow-Bertelloni, C. (2002). How Mantle Slabs Drive Plate Tectonics. Science, 298 (5591), 207–09.

Doglioni, C. (1990). The global tectonic pattern. Journal of Geodynamics, 12, 21-38.

Doglioni, C. (1993). Geological evidence for a global tectonic polarity. Journal of the Geological Society of London, 150, 991-1002.

Doglioni, C., and Panza, G. (2015). Polarized Plate Tectonics. Advances in Geophysics, 56, 1-168.

Driscoll, P. and Bercovic, D. (2013). Divergent evolution of Earth and Venus: Influence of degassing, tectonics, and magnetic fields. Icarus. 226, 1447-1464.

Egbert, G. D., Ray, R.D. (2000). Significant dissipation of tidal energy in the deep ocean inferred from satellite altimeter data. Nature, 405, 775-778.

Elsasser, W. M. (1971). Sea-floor spreading as thermal convection, J. geophys. Res., 76, 1101-1112.

Fjeldskaar, W. (1994). Viscosity and thickness of the asthenosphere detected from the Fennoscandian uplift. Earth and Planetary Science Letters, 126, 399-410.

Forster, T. D. (1969). Convection in a variable viscosity fluid heated from within. J. Geophys. Res., 74, 685-693.

Forsyth, D. & Uyeda, S. (1975). On the relative importance of the driving forces of plate motion. Geophys. J. Int., 43, 163-200.

Foulger, G. R., et, al. (2001). Seismic tomography shows that upwelling beneath Icealand is confined to the upper mantle. Geophys. J. Int., 146, 504-530.

Gerya, T. (2010). Dynamical Instability Produces Transform Faults at Mid-Ocean Ridges. Science, 329, 1047–1050.

Gerya, T. (2012). Origin and models of oceanic transform faults. Tectonophysics, 522-523, 34-54.

Giunchi, C., Spada, G., and Sabadini, R. (1997). Lateral viscosity variations and post-glacial rebound: Effects on present-day VLBI baseline deformations. Geophysical Research Letters, 24, 13-16.

Gordon, R.G. (1995). Present plate motions and plate boundaries, in Arhens, T.J., ed., Global Earth physics, Reference Shelf 1: Washington, D.C., American Geophysical Union, p. 66-87.

Gripp, A. E., and Gordon, R.G. (2002). Young tracks of hot spots and current plate velocities. Geophysical Journal International, 150, 321-361.

Gutenberg, B. (1956). The energy of Earthquakes. Quart. J. Geol. Soc. London, 112, 1-14.

Hager, B. H., and O'Connel, R. (1981). A simple global model of plate dynamics and mantle convection. Journal of Geophysical Research. 86, 4843-4867.

Hager, B. H., and Richards, M. A. (1989). Long-wavelength variations in Earth's geoid: Physical models and dynamical implications. Philosophical Transactions of the Royal Society of London, Series A, 328, 309-327.

Hales, A. (1936). Convection currents in the Earth. Monthly Notice of the Royal Astronomical Society, Geophysical Supplement, 3, 372-379.

Hess, H. H. (1962). History Of Ocean Basins, in Engel, A. E. J., James, H. L., & Leonard, B. F., eds. Petrologic Studies: A volume in honor of A. F. Buddington. Boulder, CO, Geological Society of America, 599-620.

Hilairet, N., Reynard, B., Wang, Y., et al. (2007). High-pressure creep of serpentine, interseismic deformation, and initiation of subduction. Science, 318(5858), 1910-1913.

Hirth, G. and Kohlstedt, D. (1996). Water in the oceanic upper mantle: Implications for rheology, melt extraction and the evolution of the lithosphere. Earth and Planetary Science Letters, 144, 93-108.

Holmes, A. (1931). Radioactivity and Earth Movements. Nature, 128, 496-496.

James, T. S., Gowan, E. J., Wada, L., and Wang, K. L. (2009). Viscosity of the asthenosphere from glacial isostatic adjustment and subduction dynamics at the northern Cascadia subduction zone, British Columbia, Canada. Journal of Geophysical Research: Solid Earth,114(B4), CiteID B04405.

Jeffreys, H. (1929). The Earth,2 nde d., p. 304, Cambridge University Press, London.

Jeffreys, H. (1975). The Earth. Cambridge, Cambridge University Press, pp. 1-420.

Jordan, T. H. (1974). Some comments on tidal drag as a mechanism for driving plate motions. J. Geophys. Res., 79, 2141-2142.

King, S. D. (1995). The viscosity structure of the mantle. In Reviews of Geophysics (Supplement) U.S. Quadrennial Report to the IUGG 1991-1994, 11-17.

Knopoff, L., and Leeds, A. (1972). Lithospheric momenta and the deceleration of the Earth. Nature, 237, 93-95.

Korenaga, J. (2007). Thermal cracking and the deep hydration of oceanic lithosphere: A key to the generation of plate tectonics? Journal of Geophysical Research 112(B5), DOI: 10.1029/2006JB004502.

Landuyt, W. and Bercovici, D. (2009). Variations in planetary convection via the effect of climate on damage. Earth and Planetary Science Letter, 277, 29-37.

Lenardic, A., Jellinek, M., and Moresi, L-N. (2008). A climate change induced transition in the tectonic style of a terrestrial planet. Earth and Planetary Science Letters, 271, 34-42.

Lenardic, A. and Kaula, W. (1994). Self-lubricated mantle convection: Two-dimensional models. Geophysical Research Letters, 21, 1707-1710.

Le Pichon, X. (1968). Sea-floor spreading and continental drift. Journal of Geophysical Research, 73, 3661-3697.

McKenzie, D. P. (1969). Speculations on the consequences and causes of plate motions. Geophys. J. R. astr. Soc., 18, 1-32.

McClay, K., Khalil, S. (1998). Extensional hard linkages, eastern Gulf of Suez, Egypt. Geology, 26, 563-566.

Middleton, G.V., Wilcock, P. R. (1996). Mechanics in the Earth and Environmental Sciences. Cambridge University Press, Australia : pp 496.

Miller, G. R. (1966). The flux of tidal energy out of the deep oceans. J. Geophys. Res., 71, 2485-2489.

Minster, J. B., Jordan, T. H., Molnar, P., Haines, E. (1974). Numerical modelling of instantaneous plate tectonics. Geophys. J. 36(3), 541-576.

Mitrovica, J. X. (1996). Haskell (1935) revisited. Journal of Geophysical Research, 101, 555-569.

Moore, G. W. (1973). Westward tidal lag as the driving force of plate tectonics. Geology, 1, 99-101.

Morgan, W. J. (1972). Deep mantle convection plumes and plate motions. Bull. A. Pet. Geol., 56, 203-213.

Munk, W. (1968). Once again-tidal friction. Quarterly Journal of the Royal Astronomical Society, 9, 352-375.

O'Connell, R., Gable, C.G., and Hager, B. (1991). Toroidal-poloidal partitioning of lithospheric plate motions, in Sabadini, R., et al., eds., Glacial isostasy, sea-level and mantle rheology: Dordrecht, The Netherlands, Kluwer Academic Publisher, 334, 535-551.

Oldenburg, D. W., Brune, J. N. (1972). Ridge transform fault spreading pattern in freezing wax. Science, 178, 301-304.

Oxburgh, E. and Turcotte, D. (1978). Mechanisms of continental drift. Reports on Progress in Physics, 41, 1249-1312.

Perkeris, C. (1935). Thermal convection in the interior of the Earth. Monthly Notices of the Royal Astronomical Society, Geophysical Supplement, 3, 343-367.

Piersanti, A. (1999). Postseismic deformation in Chile: Constraints on the asthenospheric viscosity. Geophysical Research Letters, 26, 3157-3160.

Pollitz, F.F., Buergmann, R., Romanowicz, B. (1998). Viscosity of oceanic asthenosphere inferred from remote triggering of Earthquakes. Science, 280, 1245-1249.

Pugh, D. T. (1987). Tides, Surges and Mean Sea-Level. JOHN WILEY & SONS.

Pugh, D. T. and Woodworth, P. L. (2014). Sea-Level Science: Understanding Tides, Surges Tsunamis and Mean Sea-Level Changes. Cambridge Univ. Press, Cambridge.

Ranalli, G. & Chandler, T. E. (1975). The Stress Field in the Upper Crust as determined from in situ Measurements. - Geol. Rundsch., 64, 653–74.

Ranalli, G. (2000). Westward drift of the lithosphere: not a result of rotational drag. Geophys. J. Int. 141, 535-537.

Ray, R. (2001). Tidal friction in the Earth and Ocean. Journées Luxembourgeoises de Géodynamique´JLG 89th, Nov. 12-14, http://www.ecgs.lu/.

Read, H. H. & Watson, J. (1975). Introduction to Geology. New York, Halsted, pp13-15.

Ricard, Y., Doglioni, C., and Sabadini, R. (1991). Differential rotation between lithosphere and mantle: A consequence of lateral viscosity variations. Journal of Geophysical Research, 96, 8407-8415.

Richardson, R.M., Cox, B.L. (1984). Evolution of oceanic lithosphere: A driving force study of the Nazca Plate. Journal of Geophysical Research: Solid Earth. 89 (B12), 10043-10052.

Richter, F. (1973). Dynamical models for sea-floor spreading, Rev. Geophys. Space Phys., 11, 223-287.

Riguzzi, F., et. al. (2010). Can Earth's rotation and tidal despinning drive plate tectonics?

Tectonophysics, 484, 60-73.

Rittmann, A. (1942). Zur thermodynamik der orogenese. Geologische Rundschau, 33, 485-498.

Rochester, M. G. (1973). The Earth's rotation, EOS, T rans. Am. geophys. Un., 54, 769-780.

Runcorn, S. (1962a).Towards a theory of continental drift. Nature,193, 311-314.

Runcorn, S. (1962b). Convection currents in the Earth's mantle. Nature, 195, 1248-1249.

Scoppola, B., Boccaletti, D., Bevis, M., Carminati, E., Doglioni, C. (2006). The westward drift of the lithosphere: a rotational drag? Bull. Geol. Soc. Am. 118 (1/2), 199-209.

Sharp, W. D. and Clague, D. A. (2006). 50-Ma Initiation of Hawaiian–Emperor bend records major change in Pacific plate motion. Science, 313(5791): 1281-1284.

Sleep, N. H. & Toksoz, M. N. (1971). Evolution of marginal basins, Nature, 233, 548-550.

Spence, W. (1987). Slab pull and the seismotectonics of subducting lithosphere. Reviews of Geophysics, 25 (1), 55–69.

Stein, C., Schmalzl, J., Hansen, U. (2004). The effect of rheological parameters on plate behavior in a self-consistent model of mantle convection. Physics of the Earth and Planetary Interiors, 142, 225-255.

Sykes, L. R. (1967). Mechanism of earthquakes and nature of faulting on the mid-oceanic ridges. J. geophys, Res., 72, 2131-2153.

Tackley, P. (1998). Self-consistent generation of tectonic plates in three-dimensional mantle convection. Earth and Planetary Science Letters, 157, 9-22.

Tanimoto, T., Lay, T. (2000). Mantle dynamics and seismic tomography. Proceedings of the National Academy of Sciences, 97 (23),12409–12410.

Tozer, D. (1985). Heat transfer and planetary evolution. Geophysical Surveys, 7, 213-246.

Trompert, R., Hansen, U. (1998). Mantle convection simulations with reheologies that generate plate-like behavior. Nature, 395, 686-689.

Turcotte, D. L., and Oxburgh, E. (1972). Mantle convection and the new global tectonics. Annual Review of Fluid Mechanics, 4, 33-66.

Turcotte, D. L., Schubert, G. (2002). Plate Tectonics. Geodynamics (2 ed.). Cambridge University Press. pp.1-21. ISBN 0-521-66186-2.

Vine, F. J., & Matthews, D. H. (1963). Magnetic Anomalies Over Oceanic Ridges. Nature, 199, 947-949.

Wegener, A. (1915). The Origin of Continents and Oceans. New York, NY: Courier Dover Publications.

Wegener, A. (1924). The origin of continents and oceans (Entstehung der Kontinente und Ozeane). Methuen & Co.

Weinstein, S. (1998). The effect of convection planform on the toroidal-poloidal energy ratio. Earth and Planetary Science Letters, 155, 87-95.

Wessel, P. & Kroenke, L.W. (2008). Pacific absolute plate motion since 145 Ma: An assessment of the fixed hot spot hypothesis. Journal of Geophysical Research - Solid Earth 113(B6). http://dx.doi.org/10.1029/2007JB005499.

White, R., McKenzie, D. (1989). Magmatism at rift zones: The generation of volcanic continental margins and flood basalts. Journal of Geophysical Research, 94, 7685-7729.

Wilson, J. T. (1965). A new class of faults and their bearing on continental drift. Nature, 207, 343-347.

Wilson, J. T., Burke, K. (1973). Plate tectonics and plume mechanics. EOS, Trans. Am. geophys, Un., 54, 238-239.

Zoback, M. L., et al. (1989). Global patterns of tectonic stress. Nature, 341, 291-298.

Zoback, M. L. (1992). First- and Second-Order Patterns of Stress in the Lithosphere:The World Stress Map Project. Journal of geophysical research, 97(B8),11703-11728.